Two-loop soft anomalous dimension matrix and resummation at next-to-next-to-leading poles

S. Mert Aybat,[1] Lance J. Dixon,[2] and George Sterman[1]

[1]*C. N. Yang Institute for Theoretical Physics, Stony Brook University, SUNY, Stony Brook, New York 11794-3840, USA*

[2]*Stanford Linear Accelerator Center, Stanford University, Stanford, California 94309, USA*

(Received 28 July 2006; published 10 October 2006)

We extend the resummation of dimensionally regulated amplitudes to next-to-next-to-leading poles. This requires the calculation of two-loop anomalous dimension matrices for color mixing through soft gluon exchange. Remarkably, we find that they are proportional to the corresponding one-loop matrices. Using the color-generator notation, we reproduce the two-loop single-pole quantities $\mathbf{H}^{(2)}$ introduced by Catani for quark and gluon elastic scattering. Our results also make possible threshold and a variety of other resummations at next-to-next-to-leading logarithm. All of these considerations apply to $2 \to n$ processes with massless external lines.

DOI: 10.1103/PhysRevD.74.074004 PACS numbers: 12.38.Cy, 11.15.Bt, 12.38.Bx, 12.39.St

I. INTRODUCTION

The description of partonic hard scattering in quantum chromodynamics (QCD) is central to the analysis of final states at hadronic colliders. The calculation of cross sections for such processes requires a combination of virtual and real radiative corrections, organized according to underlying factorization theorems. This is the case for higher-order calculations to next-to-leading or next-to-next-to-leading order in α_s (NLO, NNLO, ...). It holds as well for resummed cross sections, in which selected corrections associated with soft and collinear gluon radiation are organized, at leading, next-to-leading, or next-to-next-to-leading logarithms (LL, NLL, NNLL, ...) to all orders in α_s.

In both fixed-order and resummed calculations, the coherence properties of soft gluon radiation play an essential role. An anomalous dimension matrix for inclusive wide-angle soft gluon radiation was introduced in Refs. [1,2] and computed to leading order for quark and gluon scattering processes in Ref. [3]. The one-loop matrix of soft anomalous dimensions has been applied to the NLL threshold resummation of jet cross sections [4,5] and of distributions of event-shape variables [6,7] that are ''global'' in the sense of Ref. [8]. At two loops, the same matrix, combined with resummed form factors, was shown in Ref. [9] to control the single infrared poles of dimensionally regularized partonic scattering amplitudes in $\varepsilon = 2 - D/2$. In this paper we will show how to compute this matrix directly at two loops, from a relatively limited set of diagrams in the eikonal approximation, using Wilson lines, giving as an explicit example quark-antiquark scattering.

The full analysis given below applies to any $2 \to n$ partonic amplitude in dimensional regularization. The two-loop soft anomalous dimension matrix allows the exponentiation of next-to-next-to-leading infrared poles, which appear in the combination $\alpha_s^n (1/\varepsilon)^{n-1}$ in the exponent, a level equivalent to next-to-next-to-leading logarithms. The resulting resummed amplitudes can be expanded out to the two-loop order, and the poles in ε can be compared to explicit two-loop scattering amplitudes, for example, the basic $2 \to 2$ scattering processes [10–12]. Those poles were expressed in terms of the color-space notation [13] and the organization of two-loop singular terms presented in Ref. [14]. (Related work at one loop was performed in Refs. [15,16].) We will verify that the expansion of the resummed amplitudes to two loops matches precisely the full infrared pole structure of the known two-loop scattering amplitudes, including the single poles in ε. Remarkably, we will find, as reported in Ref. [17], that the two-loop anomalous dimension matrix is related to the one-loop matrix by a constant, the same constant, K, appearing in the DGLAP splitting kernel, that relates the one- and two-loop anomalous dimensions for the Sudakov form factor. (The analogous matrix appears in the electroweak Sudakov corrections to four-fermion scattering, and has been extracted at two loops from the QCD four-quark scattering amplitude in Ref. [18].) The simplicity of this result will facilitate the development of practical resummed cross sections with color exchange at NNLL.

This paper is organized as follows. The next section reviews the collinear and infrared factorization of exclusive amplitudes. In that section, we provide a new explicit scale-setting choice for the soft function, which is necessary to define the scales of logarithms in the relevant anomalous dimensions. The third section describes the expansion of the jet functions to two loops. Here we describe a new ''minimal'' reorganization of the factorized amplitude, to facilitate the comparison to fixed-order calculations. In the fourth section, we describe in detail the one- and two-loop calculations necessary to determine the soft anomalous dimension matrix, for the specific case of quark-antiquark scattering. Here, we will employ the eikonal approximation, and the scale-setting choice for the soft function from Sec. II. We show that diagrams attaching gluons to three different eikonal lines either vanish or represent the exponentiation of the one-loop soft matrix. We close Sec. IV by generalizing these calculations to

arbitrary flavors for incoming partons and arbitrary flavors and numbers of outgoing partons. To do so, we present the color-mixing anomalous dimension matrix in the color-space notation of Refs. [13,14]. Finally, in Sec. V we employ this notation, along with the results of Sec. IV for the soft anomalous dimensions and known two-loop elastic form factors for quarks and gluons, to give the explicit form of the two-loop single-pole terms in ε, for arbitrary $2 \to n$ partonic processes in QCD. We show that these pole terms agree with the single-pole "$\mathbf{H}^{(2)}$" terms found in NNLO $2 \to 2$ calculations [10–12,19] whose poles have been organized according to the formalism of Ref. [14]. Our results also agree with the proposal of Ref. [20] for the single poles for the case of $2 \to n$ gluon processes, which was based on the consistency of collinear factorization of amplitudes. We provide an appendix with explicit forms of Sudakov anomalous dimensions, and two appendixes illustrating calculations of soft anomalous dimensions using eikonal methods. The final appendix details the computation of a particular commutator of color-space matrices, which is needed to compare our results with the explicit NNLO calculations.

II. FACTORIZED AMPLITUDES IN DIMENSIONAL REGULARIZATION

Our considerations apply to $2 \to n$ scattering processes, denoted as "f,"

$$\mathrm{f}: f_1(p_1, r_1) + f_2(p_2, r_2) \to f_3(p_3, r_3) + f_4(p_4, r_4) + \cdots + f_{n+2}(p_{n+2}, r_{n+2}). \tag{2.1}$$

The labels f_i refer to the flavor of the participating partons, each of momenta $\{p_i\}$ and color $\{r_i\}$. The amplitude for this process, $\mathcal{M}^{[\mathrm{f}]}$, is a color tensor with indices associated with the external partons $\{r_i\} = \{r_1, r_2, \ldots\}$. It is convenient to express these amplitudes in a basis of C independent color tensors, $(c_I)_{\{r_i\}}$, so that [3,14]

$$\mathcal{M}^{[\mathrm{f}]}_{\{r_i\}}\left(\beta_j, \frac{Q^2}{\mu^2}, \alpha_s(\mu^2), \varepsilon\right) = \sum_{L=1}^{C} \mathcal{M}^{[\mathrm{f}]}_{L}\left(\beta_j, \frac{Q^2}{\mu^2}, \alpha_s(\mu^2), \varepsilon\right)(c_L)_{\{r_i\}} = |\mathcal{M}_{\mathrm{f}}\rangle, \tag{2.2}$$

where the ket may be thought of as a vector $\mathcal{M}^{[\mathrm{f}]}_{L}$ with C elements in the space of color tensors c_I. We will analyze these amplitudes at fixed momenta p_i for the participating partons, which we represent as

$$p_i = Q\beta_i, \qquad \beta_i^2 = 0, \tag{2.3}$$

where the β_i are four-velocities, and where Q is an overall momentum scale. For the purposes of this analysis, and to compare with existing NNLO calculations, we take all of the partons massless, as indicated. To be specific, we may take $\beta_1 \cdot \beta_2 = 1$ for the incoming partons in Eq. (2.1), which implies $Q^2 = s/2$, but this is not necessary.

In dimensional regularization ($D = 4 - 2\varepsilon$), on-shell amplitudes may be factorized into jet, soft, and hard functions, which describe the dynamics of partons collinear with the external lines, soft exchanges between those partons, and the short-distance scattering process, respectively. This factorization follows from the general space-time structure of long-distance contributions to elastic processes [21]. A formal proof for the case $n = 2$ in QCD (quark-quark scattering) was presented long ago [1].

The general form of the factorized amplitude is

$$\mathcal{M}^{[\mathrm{f}]}_{L}\left(\beta_i, \frac{Q^2}{\mu^2}, \alpha_s(\mu^2), \varepsilon\right) = J^{[\mathrm{f}]}\left(\frac{Q'^2}{\mu^2}, \alpha_s(\mu^2), \varepsilon\right) \times S^{[\mathrm{f}]}_{LI}\left(\beta_i, \frac{Q'^2}{\mu^2}, \frac{Q'^2}{Q^2}, \alpha_s(\mu^2), \varepsilon\right) \times H^{[\mathrm{f}]}_{I}\left(\beta_i, \frac{Q^2}{\mu^2}, \frac{Q'^2}{Q^2}, \alpha_s(\mu^2)\right), \tag{2.4}$$

where μ is the renormalization scale. $J^{[\mathrm{f}]}$ is the product of jet functions for each of the external partons, as above denoted collectively by [f], $S^{[\mathrm{f}]}$ is the soft function, and $H^{[\mathrm{f}]}$ is the short-distance function. For example, when the process is $1 + 2 \to 3 + 4$, the product of jet functions is

$$J^{[\mathrm{f}]}\left(\frac{Q'^2}{\mu^2}, \alpha_s(\mu^2), \varepsilon\right) \equiv \prod_{i=1,2,3,4} J^{[i]}\left(\frac{Q'^2}{\mu^2}, \alpha_s(\mu^2), \varepsilon\right). \tag{2.5}$$

Construction of the soft and jet functions requires the specification of at least one independent momentum scale, Q', which plays the role of a factorization scale. Such a scale, distinct from Q and μ, may be useful when one or more invariants obey strong ordering. Here, however, we shall consider "fixed-angle" scattering configurations, in which the parameter Q sets the scale for all invariants, up to numbers of order unity. With this in mind, we will simplify Eq. (2.4) somewhat, and pick $Q' = \mu$, that is, equal factorization and renormalization scales. Both the soft and jet functions then depend on $\alpha_s(\mu^2)$ only, and we will suppress their Q'^2 dependence, now expressing the same amplitude as

$$\mathcal{M}^{[\mathrm{f}]}_{L}\left(\beta_i, \frac{Q^2}{\mu^2}, \alpha_s(\mu^2), \varepsilon\right) = J^{[\mathrm{f}]}(\alpha_s(\mu^2), \varepsilon) \times S^{[\mathrm{f}]}_{LI}\left(\beta_i, \frac{Q^2}{\mu^2}, \alpha_s(\mu^2), \varepsilon\right) \times H^{[\mathrm{f}]}_{I}\left(\beta_i, \frac{Q^2}{\mu^2}, \alpha_s(\mu^2)\right), \tag{2.6}$$

that is, we suppress dependence on those variables that are set to unity by our choice of scales.

Clearly, any jet-soft-hard factorization of the sort described above is unique only up to finite factors in the various functions. There is an additional ambiguity between the jet and soft functions at the level of a single infrared pole per loop in dimensional regularization. In the remainder of this section, we will provide specific definitions for the jet and soft functions that will enable us to define and resum them unambiguously, and which will be useful in our calculations below. We begin with the jet functions.

A. The jet functions and the Sudakov form factor

The factorization (2.4) holds for any exclusive amplitude, including the elastic, or Sudakov, form factor. A very natural definition of the jet functions is, therefore, the square root of the form factor [9]. Here, we will choose the case of the elastic scattering form factor with a color-singlet source, and spacelike momentum transfer. Reverting to the general case of jet momentum scale Q'^2, not necessarily equal to the renormalization scale, this is

$$J^{[i]}\left(\frac{Q'^2}{\mu^2}, \alpha_s(\mu^2), \varepsilon\right) = J^{[\bar{i}]}\left(\frac{Q'^2}{\mu^2}, \alpha_s(\mu^2), \varepsilon\right) = \left[\mathcal{M}^{[i\to i]}\left(\frac{Q'^2}{\mu^2}, \alpha_s(\mu^2), \varepsilon\right)\right]^{1/2}. \tag{2.7}$$

Below, we shall take μ as the $\overline{\rm MS}$ renormalization scale, $\mu^2 = \mu_0^2 \exp[-\varepsilon(\gamma_E - \ln(4\pi))]$. With this choice, we may rely on the explicit form of the quark spacelike electromagnetic Sudakov form factor in $D = 4 - 2\varepsilon$ dimensions. A similar definition may be given for gluon jets in terms of matrix elements of conserved, singlet operators. In either case, the all-orders expression for the (square root of the) resummed form factor, organizing all pole terms, and implicitly specifying all finite terms of the jet defined as in Eq. (2.7), is [22–24]

$$J^{[i]}\left(\frac{Q'^2}{\mu^2}, \alpha_s(\mu^2), \varepsilon\right) = \exp\left\{\frac{1}{4}\int_0^{Q'^2}\frac{d\xi^2}{\xi^2}\left[\mathcal{K}^{[i]}(\alpha_s(\mu^2), \varepsilon) + \mathcal{G}^{[i]}\left(-1, \bar{\alpha}_s\left(\frac{\mu^2}{\xi^2}, \alpha_s(\mu^2), \varepsilon\right), \varepsilon\right) + \frac{1}{2}\int_{\xi^2}^{\mu^2}\frac{d\tilde{\mu}^2}{\tilde{\mu}^2} \times \gamma_K^{[i]}\left(\bar{\alpha}_s\left(\frac{\mu^2}{\tilde{\mu}^2}, \alpha_s(\mu^2), \varepsilon\right)\right)\right]\right\}, \tag{2.8}$$

where we use a notation for the running coupling that emphasizes its reexpansion in terms of the coupling at fixed scale μ. For our purposes below, we shall need only the "leading" form of the running coupling,

$$\bar{\alpha}_s\left(\frac{\mu^2}{\tilde{\mu}^2}, \alpha_s(\mu^2), \varepsilon\right) = \alpha_s(\mu^2)\left(\frac{\mu^2}{\tilde{\mu}^2}\right)^{\varepsilon}\sum_{n=0}^{\infty}\left[\frac{\beta_0}{4\pi\varepsilon}\left(\left(\frac{\mu^2}{\tilde{\mu}^2}\right)^{\varepsilon} - 1\right) \times \alpha_s(\mu^2)\right]^n, \tag{2.9}$$

with the one-loop coefficient

$$\beta_0 = \frac{11}{3}C_A - \frac{4}{3}T_F n_F. \tag{2.10}$$

In the expression for the jet functions above, the choice $Q'^2 = \mu^2$ can be imposed trivially. The functions $\mathcal{K}^{[i]}$, $\mathcal{G}^{[i]}$, and $\gamma_K^{[i]}$ are anomalous dimensions that can be determined by comparison to fixed-order calculations of the Sudakov form factors for quarks and gluons. These form factors are now known in QCD up to three loops [25–27]. Notice that the coupling in the argument of $\mathcal{K}^{[i]}$ is fixed at μ, so that the integral of this term alone is not well defined at $\xi^2 = 0$ even for $D \neq 4$. This apparent divergence, however, is cancelled by contributions from the upper limit of the $\tilde{\mu}^2$ integral of the anomalous dimension $\gamma_K^{[i]}$, and relates the latter to $\mathcal{K}^{[i]}$ order by order in perturbation theory. We will provide explicit expansions for these functions in Appendix A.

B. The soft function

We will broadly follow Ref. [3] in the definition of the soft function for partonic amplitudes, although we will modify certain details in the construction. The fundamental observation of Ref. [3] is that the soft function, describing color exchange between the jets, is independent of collinear dynamics, and may be constructed from an eikonal amplitude, that is, the vacuum expectation of products of ordered exponentials. For each external parton of flavor f_i, we introduce a non-Abelian path-ordered phase operator,

$$\Phi_{v_i}^{[f_i]}(\sigma', \sigma) = P\exp\left[-ig\int_{\sigma}^{\sigma'} d\lambda v_i \cdot A^{[f_i]}(\lambda v_i)\right], \tag{2.11}$$

where $v_i^\mu \sim \beta_i^\mu$ is a four-velocity. For specific calculations at two loops, it will be useful to choose these velocities to be slightly timelike,

$$0 < v_i^2 \ll 1. \tag{2.12}$$

The "opposite moving" velocity $\bar{v}_i^\mu$ projects out the large component of v_i^μ. The gauge field $A^{[f_i]}$ is a matrix in the representation of parton i. In the construction of the soft function, we will eventually take all $v_i^2 \to 0$, or equivalently, $v_i^\mu \to \beta_i^\mu$. In perturbation theory, the operators $\Phi_{v_i}^{[f_i]}(\infty, 0)$ and $\Phi_{v_i}^{[f_i]}(0, -\infty)$ respectively generate outgoing and incoming eikonal lines in the v_i directions. The eikonal sources couple to gluons at vertices in the color representation of parton i. An essential feature of these diagrams is that they are invariant under rescalings of the velocities, $v_i \to \sigma v_i$.

We are now ready to construct eikonal multipoint amplitudes from products of ordered exponentials, tied together by the same color tensors, c_L, that appear in the expansion of the partonic amplitudes, Eq. (2.2). For the $2 \to 2$ case, $1 + 2 \to 3 + 4$, this gives

$$W^{[\mathrm{f}]}_{I\{r_k\}} = (c_L)_{\{r_k\}} W^{[\mathrm{f}]}_{LI}\left(\frac{v_i \cdot v_j}{\sqrt{v_i^2 v_j^2}}\right) = \sum_{\{d_i\}} \langle 0|\Phi^{[f_4]}_{v_4}(\infty,0)_{r_4,d_4}\Phi^{[f_3]}_{v_3}(\infty,0)_{r_3,d_3} \times (c_I)_{d_4 d_3, d_2 d_1}\Phi^{[f_1]}_{v_1}(0,-\infty)_{d_1,r_1}\Phi^{[f_2]}_{v_2}(0,-\infty)_{d_2,r_2}|0\rangle. \tag{2.13}$$

Such a product is gauge invariant. The eikonal amplitude, or web function, W depends, in general, on both the invariants $v_i \cdot v_j$ and the invariant lengths v_i^2. The basic observation of Ref. [3] is that all potentially collinear divergent ratios factorize from dependence on wide-angle radiation for eikonal as well as partonic amplitudes. We can use this factorization to isolate the soft function systematically, using only calculations in the eikonal approximation.

Because of the factorization of collinear singularities, such dependence is universal, depending only on the number and flavors of the external jets. In particular, as observed above, form factors, with two external lines and trivial color flow, generate the same collinear dependence. Thus, all collinear dependence cancels in the ratio of our four-point eikonal amplitude W_I and the product of two eikonal form factors, just as in the ratio of the four-point partonic amplitudes to the corresponding form factors. We shall define S_{LI} by this ratio. Notice that information on color flow is not affected at all by the eikonal jet functions, which, like partonic jets, are diagonal in color. Thus, we define

$$S^{[\mathrm{f}]}_{LI}\left(\frac{\beta_i \cdot \beta_j}{u_0}\right) = \lim_{v^2 \to 0} \frac{W^{[\mathrm{f}]}_{LI}(\frac{v_i \cdot v_j}{v^2})}{\prod_{i \in \mathrm{f}} [W^{(i \to i)}(\frac{u_0}{v^2})]^{1/2}}, \tag{2.14}$$

where, as above, the velocities β_i are the lightlike limits of the v_i. The denominators are eikonal versions of the elastic form factors, defined with incoming velocities v_i and outgoing $\bar{v}_i$, where $v_i^2 = \bar{v}_i^2 = v^2$ and $v_i \cdot \bar{v}_i = u_0$, with u_0 a constant of order unity, independent of i, namely

$$W^{(i \to i)}\left(\frac{u_0}{v^2}\right) = \langle 0|\Phi^{[f_i]}_{\bar{v}_i}(\infty,0)\Phi^{[f_i]}_{v_i}(0,-\infty)|0\rangle. \tag{2.15}$$

This form factor generates the square of the collinear poles associated with the eikonal jet of flavor i in W_{LI}, and hence the soft function (2.14) is free of collinear divergences. We may thus take the lightlike limit for the velocities to define the soft function in the ratio.

Equation (2.14) allows us to compute the soft function, once we determine how to choose the variable u_0, so that we may match the eikonal calculation to the partonic amplitude. We can determine the correct choice as follows.

We first reexpress Eq. (2.6) for the partonic amplitude, converting it into an expression for the soft function as a ratio analogous to Eq. (2.14),

$$S^{[\mathrm{f}]}_{LI}\left(\beta_i, \frac{Q^2}{\mu^2}, \alpha_s(\mu^2), \varepsilon\right) H^{[\mathrm{f}]}_I\left(\beta_i, \frac{Q^2}{\mu^2}, \alpha_s(\mu^2)\right) = \frac{\mathcal{M}^{[\mathrm{f}]}_L(\beta_i, \frac{Q^2}{\mu^2}, \alpha_s(\mu^2), \varepsilon)}{J^{[\mathrm{f}]}(\alpha_s(\mu^2), \varepsilon)}. \tag{2.16}$$

This simple result enables us to set the scale u_0 in the definition of the eikonal form factors of Eq. (2.14). In Eq. (2.16), S can depend on the velocities only through the ratios $\beta_i \cdot \beta_j Q^2/\mu^2$. When S is calculated in this way from the ratio of partonic quantities, Q sets the scale of all momenta in the amplitude, and μ, the factorization scale in Eq. (2.6), may be reinterpreted as the momentum transfer in the form factors that define the jet functions. When calculated from the eikonal ratio, on the other hand, S depends only on the variables $\beta_i \cdot \beta_j/u_0$. To match the soft function computed in the eikonal approximation with the partonic amplitude, we need only require

$$\frac{\beta_i \cdot \beta_j}{u_0} = \frac{Q^2 \beta_i \cdot \beta_j}{\mu^2} \quad \to \quad u_0 = \frac{\mu^2}{Q^2}. \tag{2.17}$$

This relation will be used in our explicit calculations later. We are now ready to provide an all-orders expression for the soft function, analogous to Eq. (2.8) for the jet functions.

C. Resumming the soft function

We will use the $\overline{\mathrm{MS}}$ scheme for renormalization throughout. Before renormalization, all of the purely eikonal amplitudes discussed in the previous subsection give (only) scaleless integrals in perturbation theory. Such integrals vanish identically in dimensional regularization. In fact, these functions are only nontrivial because of renormalization, with every infrared pole resulting from the subtraction of a corresponding ultraviolet pole. This is the case whether or not W is collinear-regulated by introducing masses for its eikonal phases.

Thus, for both the web function W and the soft function S, we have (suppressing indices)

$$W^{[\mathrm{f}]}_{\mathrm{bare}} = 1 = Z_{W_{\mathrm{f}}}(\alpha_s(\mu), \varepsilon) W^{[\mathrm{f}]}_{\mathrm{ren}}, \qquad S^{[\mathrm{f}]}_{\mathrm{bare}} = 1 = Z_{S_{\mathrm{f}}}(\alpha_s(\mu), \varepsilon) S^{[\mathrm{f}]}_{\mathrm{ren}}, \tag{2.18}$$

and similarly for the eikonal form factors in the ratio (2.14). Both S and W are therefore defined entirely by their anomalous dimension matrices,

$$(\Gamma_A)_{IJ} = (Z_A^{-1})_{IK} \frac{d(Z_A)_{KJ}}{d\ln\mu} = (Z_A^{-1})_{IK} \beta(g,\varepsilon) \frac{\partial (Z_A)_{KJ}}{\partial g}, \tag{2.19}$$

which are given in any minimal scheme by the residues $Z_{A,1}^{(k)}$, with $A = W_{\rm f}$ or $S_{\rm f}$, of single ultraviolet poles in $1/\varepsilon$, at kth order in the expansion

$$Z_A = 1 + \sum_{k=1}^{\infty} \left(\frac{\alpha_s}{\pi}\right)^k Z_A^{(k)}(\varepsilon) = \sum_{k=1}^{\infty} \left(\frac{\alpha_s}{\pi}\right)^k \sum_{n=1}^{k} Z_{A,n}^{(k)} \left(\frac{1}{\varepsilon}\right)^n. \tag{2.20}$$

Then, for example, from the one-loop bare integrals we find the one-loop anomalous dimension from the residues of the one-loop single ultraviolet poles,

$$\Gamma_A^{(1)} = -2 Z_{A,1}^{(1)}, \tag{2.21}$$

where $\Gamma_A^{(n)}$ is the nth-order coefficient of $(\alpha_s/\pi)^n$ in Γ_A. Similarly, to order $\mathcal{O}(\alpha_s^2)$, after one-loop renormalization we find the two-loop anomalous dimensions from the two-loop single poles,

$$\Gamma_A^{(2)} = -4 Z_{A,1}^{(2)}. \tag{2.22}$$

From the definition of S, Eq. (2.14), the soft anomalous dimension matrix is found from the matrix for the corresponding eikonal amplitude by simply subtracting the anomalous dimensions for the eikonal jets. We denote the latter by $\Gamma_2^{[i]}(u_0/v^2, \alpha_s)$, and write

$$\Gamma_{S_{\rm f},IJ}\left(\frac{\beta_i\cdot\beta_j}{u_0}, \alpha_s\right) = \lim_{v^2\to 0}\left[\Gamma_{W_{\rm f},IJ}\left(\frac{v_i\cdot v_j}{v^2}, \alpha_s\right) - \delta_{IJ}\sum_{i\in {\rm f}} \Gamma_2^{[i]}\left(\frac{u_0}{v^2}, \alpha_s\right)\right]. \tag{2.23}$$

In $\Gamma_{S_{\rm f}}$, all sensitivity to collinear dynamics, and therefore to the choice of v^2, is cancelled, and the coefficients depend only on the invariants $\beta_i\cdot\beta_j$.

The matrix renormalization group equation for the eikonal amplitude $S_{IK}^{[{\rm f}]}$ is then

$$\left(\mu\frac{\partial}{\partial\mu} + \beta(g,\varepsilon)\frac{\partial}{\partial g}\right) S_{IK}^{[{\rm f}]} = -\Gamma_{S_{\rm f},IJ}\left(\frac{\beta_i\cdot\beta_j Q^2}{\mu^2}, \alpha_s\right) S_{JK}^{[{\rm f}]}, \tag{2.24}$$

from which we can solve directly for S as a path-ordered exponential,

$$\mathbf{S}_{\rm f}\left(\frac{\beta_i\cdot\beta_j}{u_0}, \alpha_s(\mu^2), \varepsilon\right) = {\rm Pexp}\left[-\frac{1}{2}\int_0^{\mu^2}\frac{d\tilde{\mu}^2}{\tilde{\mu}^2} \times \mathbf{\Gamma}_{S_{\rm f}}\left(\frac{\beta_i\cdot\beta_j}{u_0}, \bar{\alpha}_s\left(\frac{\mu^2}{\tilde{\mu}^2}, \alpha_s(\mu^2), \varepsilon\right)\right)\right], \tag{2.25}$$

where boldface (with a subscript for flavor flow) indicates a matrix. In summary, the matrix of anomalous dimensions, and hence the soft matrix itself, can be computed order by order purely from eikonal diagrams.

III. THE JET FUNCTIONS TO TWO LOOPS

In this section, we expand the jet functions in the factorized amplitude (2.6) to fixed (second) order in α_s, in a form that is convenient for comparison to explicit partonic calculations.

To determine the jet anomalous dimensions, as well as to use the resummed forms of the jet and soft functions with fixed-order calculations, we reexpand the running coupling in terms of a coupling at fixed scale. It is important to do so consistently in dimensional regularization, using the explicit form for the running coupling, Eq. (2.9). It will also be convenient to use Eq. (2.8) as a starting point to isolate the truly universal pole terms in the logarithm of the jet function, separating them from the finite terms. To this end, we introduce the notation

$$\begin{aligned}\ln J^{[i]}(\alpha_s(\mu^2), \varepsilon) &= \sum_{n=1}^{\infty}\left(\frac{\alpha_s(\mu^2)}{\pi}\right)^n \sum_{m=1}^{n+1}\frac{E_m^{[i](n)}(\varepsilon)}{\varepsilon^m} + \sum_{n=1}^{\infty}\left(\frac{\alpha_s(\mu^2)}{\pi}\right)^n e^{[i](n)}(\varepsilon) \\ &= E^{[i]}(\alpha_s(\mu^2), \varepsilon) + e^{[i]}(\alpha_s(\mu^2), \varepsilon),\end{aligned} \tag{3.1}$$

in terms of the coupling $\alpha_s(\mu^2)$ at fixed scale μ. As in Eq. (2.6), we set the jet factorization scale $Q' = \mu$. The pure pole terms in Eq. (3.1) have been expanded at each order as

$$E^{[i](n)}(\varepsilon) \equiv \sum_{m=1}^{n+1}\frac{E_m^{[i](n)}(\varepsilon)}{\varepsilon^m}, \tag{3.2}$$

while the functions $e^{[i](n)}(\varepsilon)$ absorb all terms that remain finite for $\varepsilon = 0$, order by order in α_s. The coefficients $E_m^{[i](n)}$ and the functions $e^{[i](n)}(\varepsilon)$ are determined, of course, by the expansions of the functions γ_K, $\mathcal{K}$ and $\mathcal{G}$, which depend, in general, on the definition (2.7) of the jet. This separation, however, eliminates the remaining arbitrariness in choosing the form factor by defining a ''minimal'' jet, consisting of the exponential of pole terms only,

$$\mathcal{J}^{[i]}(\alpha_s(\mu^2), \varepsilon) \equiv \exp[E^{[i]}(\alpha_s, \varepsilon)]. \tag{3.3}$$

In this notation, we rewrite our basic factorization, Eq. (2.6), in minimal form as

$$\mathcal{M}_L^{[\mathrm{f}]}\left(\beta_i, \frac{Q^2}{\mu^2}, \alpha_s(\mu^2), \varepsilon\right) = \prod_{i\in \mathrm{f}} \mathcal{J}^{[i]}(\alpha_s(\mu^2), \varepsilon) \times S_{LI}^{[\mathrm{f}]}\left(\frac{\beta_i\cdot\beta_j Q^2}{\mu^2}, \alpha_s(\mu^2), \varepsilon\right) \times \mathcal{H}_I^{[\mathrm{f}]}\left(\beta_i, \frac{Q^2}{\mu^2}, \alpha_s(\mu^2)\right), \tag{3.4}$$

where we have absorbed the (color-diagonal) finite factors into the perturbative definition of the short-distance function

$$\mathcal{H}_I^{[\mathrm{f}]}\left(\beta_i, \frac{Q^2}{\mu^2}, \alpha_s(\mu^2), \varepsilon\right) = \exp\left[\sum_{i\in \mathrm{f}} e^{[i]}(\alpha_s(\mu^2), \varepsilon)\right] \times H_I^{[\mathrm{f}]}\left(\beta_i, \frac{Q^2}{\mu^2}, \alpha_s(\mu^2)\right). \tag{3.5}$$

We will also find it useful to write this expression in the color-state notation of Eq. (2.2), as

$$|\mathcal{M}_{\mathrm{f}}\rangle = \prod_{i\in \mathrm{f}} \mathcal{J}^{[i]}(\alpha_s(\mu^2), \varepsilon)\mathbf{S}_{\mathrm{f}}\left(\frac{\beta_i\cdot\beta_j Q^2}{\mu^2}, \alpha_s(\mu^2), \varepsilon\right)|\mathcal{H}_{\mathrm{f}}\rangle, \tag{3.6}$$

where again the matrix structure of the soft function is denoted by boldface and where we treat $\mathcal{H}_I^{[\mathrm{f}]}$ in the notation of Eq. (2.2).

Before this refactorization, the logarithm of the full jet function $J^{[i]}$ at two loops is given by

$$\ln J^{[i]}(\alpha_s(\mu^2), \varepsilon) = \frac{1}{4}\left\{-\left(\frac{\alpha_s}{\pi}\right)\left(\frac{1}{2\varepsilon^2}\gamma_K^{[i](1)} + \frac{1}{\varepsilon}\mathcal{G}^{[i](1)}(\varepsilon)\right) + \left(\frac{\alpha_s}{\pi}\right)^2\left[\frac{\beta_0}{8}\frac{1}{\varepsilon^2}\left(\frac{3}{4\varepsilon}\gamma_K^{[i](1)} + \mathcal{G}^{[i](1)}(\varepsilon)\right) - \frac{1}{2}\left(\frac{\gamma_K^{[i](2)}}{4\varepsilon^2} + \frac{\mathcal{G}^{[i](2)}(\varepsilon)}{\varepsilon}\right)\right] + \cdots\right\}. \tag{3.7}$$

To determine the coefficients $E_m^{[i](n)}$ in the minimal two-loop jet function, we only need to expand the functions $\mathcal{G}^{[i](n)}(\varepsilon)$,

$$\mathcal{G}^{[i](n)}(\varepsilon) = \mathcal{G}_0^{[i](n)} + \varepsilon\mathcal{G}^{[i](n)\prime}(0) + \cdots. \tag{3.8}$$

Explicit forms for these anomalous dimensions can be found in Appendix A. In terms of these quantities, we readily find that the full single-pole terms in the logarithm of the jet function are given at one and two loops by

$$\begin{aligned}
&E_2^{[i](1)} = -\frac{1}{8}\gamma_K^{[i](1)}, \qquad E_1^{[i](1)} = -\frac{\mathcal{G}_0^{[i](1)}}{4}, \qquad E_3^{[i](2)} = \frac{3\beta_0}{128}\gamma_K^{[i](1)}, \qquad E_2^{[i](2)} = \frac{\beta_0}{32}\mathcal{G}_0^{[i](1)} - \frac{1}{32}\gamma_K^{[i](2)},\\
&E_1^{[i](2)} = -\frac{\mathcal{G}_0^{[i](2)}}{8} + \frac{\beta_0\mathcal{G}^{[i](1)\prime}(0)}{32},\\
&E_1^{[q](2)} = -\frac{3}{8}C_F^2\left[\frac{1}{16} - \frac{1}{2}\zeta(2) + \zeta(3)\right] - \frac{1}{16}C_A C_F\left[\frac{961}{216} + \frac{11}{4}\zeta(2) - \frac{13}{2}\zeta(3)\right] + \frac{1}{16}C_F T_F n_F\left[\frac{65}{54} + \zeta(2)\right],\\
&E_1^{[g](2)} = \frac{1}{32}C_A^2\left[-\frac{346}{27} + \frac{11}{6}\zeta(2) + \zeta(3)\right] + \frac{1}{16}C_A T_F n_F\left[\frac{64}{27} - \frac{\zeta(2)}{3}\right] + \frac{1}{16}C_F T_F n_F,
\end{aligned} \tag{3.9}$$

where for $E_1^{[i](2)}$ we give the explicit expressions for the quark and gluon cases. Notice that the full single-pole term includes a contribution from the running of the finite term at one loop, which appears as an $\mathcal{O}(\varepsilon)$ contribution in $\mathcal{G}^{[i](1)}$.

IV. EIKONAL AMPLITUDES AT ONE AND TWO LOOPS

We begin this section with a calculation of the soft anomalous dimension matrix for quark-antiquark elastic scattering at one and two loops, in terms of a specific color basis [3], and then discuss the representation of the matrix in the color-generator notation of Refs. [13,14]. We will see that the basic result of our calculation, the proportionality of the one- and two-loop matrices, applies to a much wider class of processes.

A. 2 → 2 eikonal diagrams at one loop

Here we will present the calculation for one-loop corrections to W, Eq. (2.13), for quark-antiquark scattering, and by using Eq. (2.21) we will derive the corresponding one-loop soft anomalous dimension matrix. Representative one-loop diagrams are shown in Fig. 1. One can write the amplitude for any diagram D as

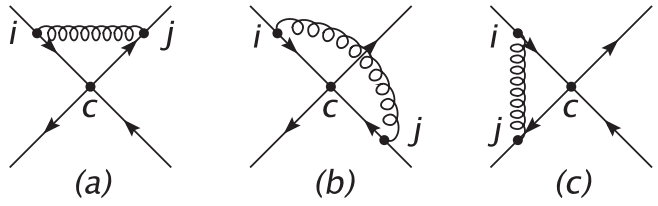

FIG. 1. One-loop diagrams that contribute to $\Gamma_{S_{\mathrm{f}}}^{(1)}$.

$$M_D = F_D \times C_{D,I}, \tag{4.1}$$

where F_D is the corresponding Feynman integral in dimensional regularization and $C_{D,I}$ is the color tensor. We will refer to F_D as the velocity factor below, because it absorbs all dependence on kinematic variables. To uniquely define the normalizations of the velocity factors, and hence the color tensors, we define them to equal the corresponding integrals for the scattering of eikonal lines that couple to the exchanged gluons via color-independent "Abelian" vertices. In particular, we absorb into the velocity factors the (-1) associated with a gluon coupled to an eikonal line in the antiquark representation. Note that this separation of color and velocity factors is possible even if the eikonal lines are in the adjoint representation. This method will facilitate our eventual comparison to results expressed in the formalism of Ref. [14].

Consider the left-hand diagram in Fig. 1, which we will call a "t-channel diagram," referring to the pair of eikonal lines to which the gluon is connected. We will follow Refs. [28,29], and express the velocity factor as an integral in configuration space. For an arbitrary one-gluon correction to a phase operator of the form of Eq. (2.13), such a correction is given by

$$F_t = (ig\mu^\varepsilon)^2 \int_{\mathcal{C}_i} dx_\mu \int_{\mathcal{C}_j} dy_\nu D^{\mu\nu}(x-y), \tag{4.2}$$

where integration is performed over the positions of gluons on the paths of the Wilson lines, $\mathcal{C}_i$ and $\mathcal{C}_j$. For the lines in Eq. (2.13) these paths are specified by

$$\mathcal{C}_i = v_i\beta, \qquad \mathcal{C}_j = v_j\alpha, \tag{4.3}$$

where α and β run from $-\infty$ to 0 (0 to ∞) for an incoming (outgoing) path. For the t-channel diagram shown in Fig. 1(a), for example, where $t = (p_1 - p_3)^2 = (p_2 - p_4)^2$, we may have $\{i, j\} = \{1, 3\}$ or $\{2, 4\}$.

In Feynman gauge the coordinate-space gluon propagator, in dimensional regularization with $D = 4 - 2\varepsilon$, is given by [29]

$$D_{\mu\nu}(x) = g_{\mu\nu}D(x) = g_{\mu\nu}\frac{\Gamma(1-\varepsilon)}{4\pi^{2-\varepsilon}}\frac{1}{(x^2 - i\epsilon)^{1-\varepsilon}}. \tag{4.4}$$

Using this expression in Eq. (4.2), we have

$$\begin{aligned} F_t &= (ig\mu^\varepsilon)^2 \int_0^\infty d\alpha \int_{-\infty}^0 d\beta\, v_i^\mu D_{\mu\nu}(v_j\alpha - v_i\beta)v_j^\nu \\ &= (ig\mu^\varepsilon)^2 (v_i \cdot v_j)\frac{\Gamma(1-\varepsilon)}{4\pi^{2-\varepsilon}} \\ &\quad \times \int_0^\infty d\alpha \int_0^\infty d\beta \frac{1}{[(v_j\alpha + v_i\beta)^2 - i\epsilon]^{1-\varepsilon}}. \end{aligned} \tag{4.5}$$

As observed above, all such integrals vanish in dimensional regularization, since they are scaleless. The contribution of each such velocity-dependent integral is given by its counterterm, equal to its infrared pole and hence to the negative of its ultraviolet (UV) pole. Of course, F_t may be evaluated as a momentum-space integral with equivalent results.

In order to isolate the (single) UV pole in Eq. (4.5), we apply an infrared cutoff for the integral by introducing a small parameter λ with units of mass. This can be effected simply by inserting $\theta(1/\lambda - \alpha)$ in Eq. (4.5). The α and β integrals are then easily related to a single integral in terms of $z = \frac{\alpha}{(\alpha+\beta)}$ [see Eq. (B3) in Appendix B]. We find

$$\begin{aligned} F_t &= -\left(\frac{\alpha_s}{\pi}\right)\left(\frac{\pi\mu^2}{\lambda^2}\right)^\varepsilon \Gamma(1-\varepsilon)\frac{1}{2\varepsilon} \\ &\quad \times \int_0^1 dz \frac{v_i \cdot v_j}{([v_j z + v_i(1-z)]^2)^{1-\varepsilon}}. \end{aligned} \tag{4.6}$$

The single UV pole term in this expression is given by [28,29]

$$F_t^{s.p.}(v_i, v_j) = -\left(\frac{\alpha_s}{\pi}\right)\frac{1}{2\varepsilon}\gamma_{ij}\coth\gamma_{ij}, \tag{4.7}$$

where

$$\cosh\gamma_{ij} \equiv \frac{v_i \cdot v_j}{\sqrt{v_i^2 v_j^2}}. \tag{4.8}$$

Because there is only a single, overall infrared divergence in F_t, any such cutoff will give the same ultraviolet pole.

In the high-energy limit ($\gamma_{ij} \gg 1$), we have

$$F_t^{s.p.}(v_i, v_j) = -\left(\frac{\alpha_s}{\pi}\right)\frac{1}{2\varepsilon}\gamma_{ij}. \tag{4.9}$$

For $\{i, j\} = \{1, 3\}$ and $\{i, j\} = \{2, 4\}$ the answers are identical, in this $2 \to 2$ process. In the high-energy limit we define

$$\begin{gathered} \gamma_{13} = \gamma_{24} = T, \qquad \gamma_{14} = \gamma_{23} = U, \\ \gamma_{12} = \gamma_{34} = S, \end{gathered} \tag{4.10}$$

where

$$\begin{aligned} T &= \ln\left(\frac{2v_1 \cdot v_3}{v^2}\right) = \ln\left(\frac{2v_2 \cdot v_4}{v^2}\right), \\ U &= \ln\left(\frac{2v_1 \cdot v_4}{v^2}\right) = \ln\left(\frac{2v_2 \cdot v_3}{v^2}\right), \\ S &= \ln\left(\frac{-2v_1 \cdot v_2}{v^2}\right) = \ln\left(\frac{-2v_3 \cdot v_4}{v^2}\right), \end{aligned} \tag{4.11}$$

with $v_i^2 \equiv v^2$ for all i. The velocity factors for u- and s-channel diagrams are found by taking into account the extra minus sign associated with coupling to an eikonal line in the antiquark representation, as well as that from crossing substitutions, which change the sign of $\coth\gamma_{ij}$ from unity to -1 in the high-energy limit,

$$F_u(v_i, v_j) = -F_t(v_i, v_j), \qquad F_s(v_i, v_j) = F_t(v_i, -v_j). \tag{4.12}$$

Here, $\{i, j\} = \{1, 4\}$ and $\{2, 3\}$ for the u-channel diagrams, and $\{i, j\} = \{1, 2\}$ and $\{3, 4\}$ for the s-channel diagrams. The function F_s has the same overall sign as F_t because it differs both by an antiquark connection and by crossing, while F_u has the opposite sign.

In summary, the single poles for the velocity factors for the diagrams in Fig. 1 are given by

$$F_t^{s.p.} = -\left(\frac{\alpha_s}{\pi}\right)\frac{1}{2\varepsilon}T, \qquad F_u^{s.p.} = \left(\frac{\alpha_s}{\pi}\right)\frac{1}{2\varepsilon}U, \qquad F_s^{s.p.} = -\left(\frac{\alpha_s}{\pi}\right)\frac{1}{2\varepsilon}S. \tag{4.13}$$

To construct the counterterms, of course, we must also compute the corresponding color tensors for each diagram.

We will use $C_i^{[t]}$ to denote the color tensor for the t-channel diagram in Fig. 1, with color tensor c_i, $i = 1, 2$ at short distances. For the latter, we choose the basis tensors shown in Fig. 2. The coefficients of the color tensors absorb all overall factors not included in the velocity factors of Eq. (4.13).

One can calculate these color tensors from the basic identity for the generators of SU(N_c),

$$\sum_a (T^a)_{r_2 r_1}(T^a)_{r_3 r_4} = \frac{1}{2}\delta_{r_2 r_4}\delta_{r_3 r_1} - \frac{1}{2N_c}\delta_{r_2 r_1}\delta_{r_3 r_4}. \tag{4.14}$$

In the color basis given in Fig. 2, the color tensors of the t-channel diagrams are given by

$$C_1^{[t]} = -\frac{1}{2N_c}c_1 + \frac{1}{2}c_2, \qquad C_2^{[t]} = \frac{N_c^2 - 1}{2N_c}c_2 = C_F c_2. \tag{4.15}$$

We will employ a similar notation below for other one-loop and for two-loop diagrams. Color tensors for the u- and s-channel diagrams are computed in a similar way with the results

$$C_1^{[u]} = -\frac{1}{2N_c}c_1 + \frac{1}{2}c_2, \qquad C_2^{[u]} = \frac{1}{2}c_1 - \frac{1}{2N_c}c_2, \tag{4.16}$$

and

$$C_1^{[s]} = C_F c_1, \qquad C_2^{[s]} = \frac{1}{2}c_1 - \frac{1}{2N_c}c_2. \tag{4.17}$$

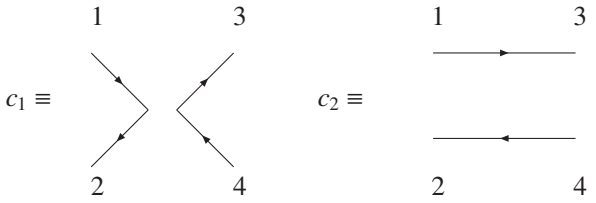

FIG. 2. Color basis $\{c_1, c_2\}$ for the four-quark process.

We summarize these relations in matrix form by

$$C_I^{[a]} = \sum_{J=1,2} c_J d_{JI}^{[a]}, \tag{4.18}$$

where the matrix element $d_{JI}^{[a]}$ specifies the mixing from color tensor c_I to tensor c_J by the exchange of a gluon in channel $a = t, u, s$. An important identity that we will use below is

$$d_{JI}^{[t]} + d_{JI}^{[s]} - d_{JI}^{[u]} = C_F\delta_{JI}, \tag{4.19}$$

which we easily verify from the relations above. Note that this equality holds in an arbitrary representation.[1]

The contribution of each diagram to the matrix counterterm $Z_{W_f}^{(1)}$ is now found by the product of the corresponding color factor times the pole part of the velocity factor,

$$(Z_{W_f}^{(1)})_{JI} = 2\sum_{a=s,t,u} d_{JI}^{[a]}\frac{F_a^{s.p.}}{\alpha_s/\pi}, \tag{4.20}$$

in terms of the single-pole terms of Eq. (4.13) and the color factors read off from Eqs. (4.15), (4.16), and (4.17). Given the counterterm matrix, we can evaluate $\mathbf{\Gamma}_{W_f}^{(1)}$ by using Eq. (2.21) with the result

$$\mathbf{\Gamma}_{W_f}^{(1)} = \begin{pmatrix} \frac{1}{N_c}(U - T) + 2C_F S & (S - U) \\ (T - U) & \frac{1}{N_c}(U - S) + 2C_F T \end{pmatrix}. \tag{4.21}$$

Exactly the same calculation gives $\Gamma_2^{[i]}$, the anomalous dimension for the eikonal jet function, defined as the square root of the eikonal singlet form factor, Eq. (2.15). In Eq. (4.9), we simply let $\cosh\gamma_{ij} \to u_0/v^2 = \mu^2/(Q^2 v^2)$ [using Eq. (2.17)], in the limit $v^2 \to 0$. The one-loop result for parton i is then given by

$$\Gamma_2^{[i](1)}\left(\frac{u_0}{v^2}\right) = \frac{1}{2}C_i \ln\left(\frac{\mu^2}{Q^2 v^2}\right), \tag{4.22}$$

with $C_i = C_F$ for quarks and C_A for gluons. By using this expression and the definition for Γ_{S_f}, Eq. (2.23), we find

$$\mathbf{\Gamma}_{S_f}^{(1)} = \begin{pmatrix} \frac{1}{N_c}(\mathcal{U} - \mathcal{T}) + 2C_F\mathcal{S} & (\mathcal{S} - \mathcal{U}) \\ (\mathcal{T} - \mathcal{U}) & \frac{1}{N_c}(\mathcal{U} - \mathcal{S}) + 2C_F\mathcal{T} \end{pmatrix}, \tag{4.23}$$

where

$$\mathcal{T} \equiv \ln\left(\frac{-t}{\mu^2}\right), \qquad \mathcal{U} \equiv \ln\left(\frac{-u}{\mu^2}\right), \qquad \mathcal{S} \equiv \ln\left(\frac{-s}{\mu^2}\right). \tag{4.24}$$

After performing the subtraction of the jet functions, we set

[1]Equation (4.19) is equivalent in this case to the well-known identity $\sum_i \mathbf{T}_i = 0$ in the color-generator notation that we will review below.

$v_i \to \beta_i$, and then use Eqs. (2.3) and (2.17) to recast the result in terms of the usual Mandelstam variables, t, u, and s. We notice that, as anticipated, all collinear logarithms, and hence sensitivity to our choice of collinear regulation, are absent in the soft anomalous dimension matrix, $\mathbf{\Gamma}^{(1)}_{S_f}$.

B. $2 \to 2$ eikonal diagrams at two loops

Figure 3 shows the classes of topologically inequivalent diagrams that contribute to $\Gamma^{(2)}_{S_f}$, when combined with their one-loop counterterm diagrams. One obtains the full set from all different combinations of external legs with these topologies. It is easy to see that the number of graphs for each inequivalent set is $N_a = 6$, $N_b = 6$, $N_c = 6$, $N_d = 12$, $N_e = 12$, $N_f = 12$, $N_g = 4$, $N_h = 24$, and $N_i = 3$, which in total gives 85 two-loop diagrams. As in the one-loop case, we find anomalous dimensions from the combinations of velocity factors and color tensors.

Consider first diagram (i), which is the only two-loop topology involving all four eikonal lines. Diagram (i) does not have a surviving single UV pole when we add its one-loop counterterms.

Regarding the remaining cases, we consider first those diagrams involving two eikonal lines only, which we refer to as "2E" diagrams. Next, we will show that diagram (g) vanishes, which we consider a very important result. Finally, we will calculate all the contributions from the surviving "3E" diagram type (h). In this case, we will find that the diagrams, although nonvanishing, reduce to the product of one-loop diagrams, and thus do not contribute to the two-loop anomalous dimensions.

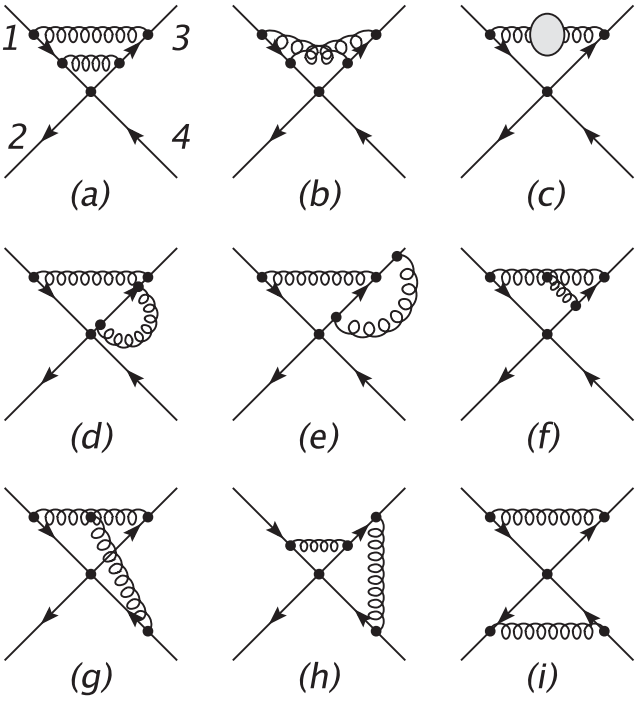

FIG. 3. Two-loop diagrams that contribute to $\Gamma^{(2)}_{W_f}$.

1. The 2E diagrams and $\Gamma^{(2)}_i$

In the 2E diagrams, (a), (b), (c), (d), (e), and (f), the gluons connect to only two of the four eikonal lines in W. These same diagrams also contribute to the two-loop cusp anomalous dimension, $\Gamma^{[i](2)}_2$, and their single UV poles are well known [29]. We review their velocity factors here, because they are needed for the two-loop anomalous dimension matrix. Additional details are given in Appendix C.

The color factors of the 2E diagrams are proportional to the color-mixing matrix elements for single t-channel gluon exchange, $d^{[t]}_{JI}$, defined in Eq. (4.18). This is manifestly the case for the individual diagrams (c), (d), (e), and (f). For the sum of diagrams (a) and (b), it relies on the result [28,29] that the single-pole terms in the velocity factors of these two diagrams are the negatives of each other. The net color factor for the (a) and (b) single poles is then proportional to the commutator of two generators, which allows it to be expressed in terms of the one-loop color factor, as $C_A d^{[t]}_{JI}$. We can thus present the contributions of all the 2E diagrams in terms of the $d^{[a]}_{JI}$, with $a = s$, t, u.

In terms of the factors $d^{[t]}_{JI}$, the two-loop counterterms[2] for the diagrams (a), (b), (c), and (f) in the high-energy limit are, analogously to the one-loop velocity factors, Eq. (4.13),

$$(Z^{(a+b)}_{W_f})_{JI} = -\left(\frac{\alpha_s}{\pi}\right)^2 d^{[t]}_{JI}\frac{C_A}{2}\frac{1}{2\varepsilon}\left[\frac{T^3}{6} + \frac{\zeta(2)}{2}T - \frac{\zeta(3)}{2}\right],$$
$$(Z^{(c)}_{W_f})_{JI} = -\left(\frac{\alpha_s}{\pi}\right)^2 d^{[t]}_{JI}\frac{1}{2}\frac{1}{2\varepsilon}\left(\frac{31}{36}C_A - \frac{5}{9}T_F n_F\right)T, \quad (4.25)$$

and

$$(Z^{(f)}_{W_f})_{JI} = -\left(\frac{\alpha_s}{\pi}\right)^2 d^{[t]}_{JI}\frac{C_A}{2}\frac{1}{4\varepsilon}\left\{\left[-\frac{T^3}{6} + (1-\zeta(2))T\right] + \left[\frac{T^2}{2} - T + \zeta(2)\right]\right\}, \quad (4.26)$$

with T the logarithm of $2v_1 \cdot v_3/v^2$, as in Eq. (4.11). In Eq. (4.26), the second term in square brackets gives the result of those numerator terms that are proportional to v_3^2 before the integration. (See Appendix C.) The entire T dependence of these terms cancels against the contributions from diagrams (d) and (e), which are also proportional to v_3^2 before integration and are given individually by

[2]These results, of course, require that we combine these diagrams with the corresponding one-loop counterterms for their divergent subdiagrams. Notice that diagram (b) in Fig. 3 does not have a one-loop counterterm since it does not have a divergent subdiagram.

$$(Z^{(d)}_{W_{\rm f}})_{JI} = -\left(\frac{\alpha_s}{\pi}\right)^2 d^{[t]}_{JI} C_F \frac{1}{4\varepsilon}\left[-\frac{T^2}{2} + T - \frac{\zeta(2)}{2}\right],$$
$$(Z^{(e)}_{W_{\rm f}})_{JI} = \left(\frac{\alpha_s}{\pi}\right)^2 d^{[t]}_{JI}\left(C_F - \frac{C_A}{2}\right)\frac{1}{4\varepsilon}\left[-\frac{T^2}{2} + T - \frac{\zeta(2)}{2}\right]. \tag{4.27}$$

The combined t-channel contribution from the six diagrams (a), (b), (c), (d), (e), and (f) to the soft anomalous dimension matrix is found by adding Eqs. (4.25), (4.26), and (4.27),[3]

$$\begin{aligned}(Z^{[t]}_{W_{\rm f}})_{JI} &\equiv 2(Z^{(a+b)}_{W_{\rm f}} + Z^{(c)}_{W_{\rm f}} + 2[Z^{(d)}_{W_{\rm f}} + Z^{(e)}_{W_{\rm f}} + Z^{(f)}_{W_{\rm f}}])_{JI} \\ &= -\frac{1}{2\varepsilon}\left(\frac{\alpha_s}{\pi}\right)^2 d^{[t]}_{JI}\left\{\left[C_A\left(\frac{67}{36} - \frac{\zeta(2)}{2}\right) - \frac{5}{9}T_F n_F\right]\right. \\ &\quad \left.\times \ln\left(\frac{2v_1\cdot v_3}{v^2}\right) + \frac{C_A}{2}(\zeta(2) - \zeta(3))\right\} \\ &= \left(\frac{\alpha_s}{\pi}\right)^2 d^{[t]}_{JI}\left\{\frac{K}{2}\frac{F_t^{s.p.}}{(\alpha_s/\pi)} - \frac{C_A}{4\varepsilon}(\zeta(2) - \zeta(3))\right\},\end{aligned} \tag{4.28}$$

where the last line recalls a standard notation [30] for the quantity K,

$$K \equiv C_A\left(\frac{67}{18} - \zeta(2)\right) - \frac{10}{9}T_F n_F. \tag{4.29}$$

The result (4.28) includes a factor of 2 for the other t-channel exchange, between lines 2 and 4.

Analogous considerations, of course, apply to diagrams with pairs of s- and u-channel 2E diagrams. Together with the t-channel diagrams, they contribute to the two-loop anomalous dimension matrix for W according to Eq. (2.22),

$$\begin{aligned}\mathbf{\Gamma}^{(2E)(2)}_{W_{\rm f}} &= K\sum_{i=s,t,u} d^{[i]}_{JI}\left(\frac{-2\varepsilon F_i^{s.p.}}{(\alpha_s/\pi)}\right) + \delta_{JI}C_A C_i(\zeta(2) - \zeta(3)) \\ &= \frac{K}{2}\mathbf{\Gamma}^{(1)}_{W_{\rm f}} + \delta_{JI}C_A C_i(\zeta(2) - \zeta(3)),\end{aligned} \tag{4.30}$$

where we have used the identity (4.19), and where $\mathbf{\Gamma}^{(1)}_{W_{\rm f}}$ is the same one-loop anomalous dimension given in Eq. (4.21).

In a precisely similar manner, we find for the two-loop form factor (cusp) anomalous dimension for partonic representation i,

$$\Gamma^{[i](2)}_2\left(\frac{u_0}{v^2}\right) = \frac{C_i}{4}\left[K\ln\left(\frac{\mu^2}{Q^2v^2}\right) + C_A(\zeta(2) - \zeta(3))\right]. \tag{4.31}$$

As at one loop, we combine Eqs. (4.30) and (4.31) in Eq. (2.23), in order to find the contribution of the 2E diagrams to the two-loop soft anomalous dimensions for scattering.

It is now clear that the two-loop soft anomalous dimension matrix inherits from the 2E diagrams a factor of K times the one-loop anomalous dimension matrix. The result is

$$\mathbf{\Gamma}^{(2E)(2)}_{S_{\rm f}} = \frac{K}{2}\mathbf{\Gamma}^{(1)}_{S_{\rm f}}, \tag{4.32}$$

with $\mathbf{\Gamma}^{(1)}_{S_{\rm f}}$ the same one-loop anomalous dimension given in Eq. (4.23). All velocity-independent terms in the $Z^{(2E)}_{W_{\rm f}}$ that are not in $\mathbf{\Gamma}^{(1)}_{S_{\rm f}}$ cancel in Eq. (2.23) against the corresponding finite terms from the eikonal form factors in the two-loop soft anomalous dimension, along with all collinear-singular dependence. This is important, because the constant terms depend, in general, on the eikonal approximation and our choice of collinear regularization. At the same time, we have now used *all* the collinear-singular dependence in the Sudakov anomalous dimensions, Eq. (4.31), to cancel the $\ln v^2$ dependence of the 2E diagrams of W. The 3E diagrams, represented by (g) and (h) in Fig. 3, have no remaining subtractions. The combination of these classes of diagrams must therefore be free of collinear singularities at the two-loop level.

2. Vanishing of three-gluon diagram with three eikonal lines

Now let us show that diagram (g) in Fig. 3 vanishes. Up to overall factors which play no role, the velocity Feynman integral for a generic three-gluon diagram can be written as

$$\begin{aligned}F(v_A, v_B, v_C) = \int d^Dk_1 d^Dk_2 &\frac{1}{v_B\cdot k_1 + i\epsilon}\frac{1}{v_A\cdot k_2 + i\epsilon} \\ &\times \frac{1}{v_C\cdot(k_1+k_2) + i\epsilon}\frac{1}{k_1^2 + i\epsilon}\frac{1}{k_2^2 + i\epsilon} \\ &\times \frac{1}{(k_1+k_2)^2 + i\epsilon}\times[v_A\cdot v_B\, v_C\cdot(k_1 - k_2) \\ &+ v_A\cdot v_C\, v_B\cdot(k_1 + 2k_2) \\ &+ v_B\cdot v_C\, v_A\cdot(-2k_1 - k_2)],\end{aligned} \tag{4.33}$$

where the term in square brackets is the three-gluon vertex momentum factor. Here v_A, v_B, and v_C are three different eikonal velocities. We take lightlike $v_A^2 = v_B^2 = 0$. We can then expand any momentum p^μ as

$$p^\mu = \frac{v_A^\mu}{v_A\cdot v_B}v_B\cdot p + \frac{v_B^\mu}{v_A\cdot v_B}v_A\cdot p + p_T^\mu, \tag{4.34}$$

with p_T^μ the transverse components, satisfying $v_A\cdot p_T = v_B\cdot p_T = 0$.

For use in the integral, we introduce the variables

$$\xi_i = \frac{v_A\cdot v_C}{v_A\cdot v_B}v_B\cdot k_i, \qquad \eta_i = \frac{v_B\cdot v_C}{v_A\cdot v_B}v_A\cdot k_i. \tag{4.35}$$

[3]Note that one needs to multiply Eqs. (4.26) and (4.27) by 2 because, for these diagrams, there are two ways of attaching the gluons to the eikonal lines.

We introduce these variables into the integral by using v_A and v_B to define light-cone coordinates,

$$dk_i^+ dk_i^- = \frac{1}{v_A \cdot v_B} d(v_B \cdot k_i) d(v_A \cdot k_i) = \frac{v_A \cdot v_B}{(v_A \cdot v_C)(v_B \cdot v_C)} d\xi_i d\eta_i, \tag{4.36}$$

so that

$$k_i^2 = 2\frac{(v_A \cdot k_i)(v_B \cdot k_i)}{v_A \cdot v_B} - k_{i,T}^2 = 2\frac{v_A \cdot v_B}{(v_A \cdot v_C)(v_B \cdot v_C)} \xi_i \eta_i - k_{i,T}^2. \tag{4.37}$$

When we change variables in F to the ξ's and η's, we find

$$\begin{aligned} F(v_A, v_B, v_C) = {} & \frac{v_A \cdot v_B}{(v_A \cdot v_C)(v_B \cdot v_C)} \int \prod_{i=1}^{2} d\xi_i d\eta_i d^{D-2} k_{i,T} \frac{1}{2\frac{v_A \cdot v_B}{(v_A \cdot v_C)(v_B \cdot v_C)} \xi_i \eta_i - k_{i,T}^2 + i\epsilon} \\ & \times \frac{1}{2\frac{v_A \cdot v_B}{(v_A \cdot v_C)(v_B \cdot v_C)} (\xi_1 + \xi_2)(\eta_1 + \eta_2) - (k_{1,T} + k_{2,T})^2 + i\epsilon} \frac{1}{\xi_1 + i\epsilon} \frac{1}{\eta_2 + i\epsilon} \\ & \times \frac{1}{\xi_1 + \xi_2 + \eta_1 + \eta_2 - v_{C,T} \cdot (k_1 + k_2)_T + i\epsilon} \\ & \times [\xi_1 - \xi_2 + \eta_1 - \eta_2 - v_{C,T} \cdot (k_1 - k_2)_T + \xi_1 + 2\xi_2 - 2\eta_1 - \eta_2] \\ = {} & 0. \end{aligned} \tag{4.38}$$

The integral vanishes because the numerator is antisymmetric under $\xi_1 \leftrightarrow \eta_2$, $\xi_2 \leftrightarrow \eta_1$, and $k_{1,T} \leftrightarrow k_{2,T}$, while the product of the denominators is symmetric. Notice that group factors play no part in this argument. This result is therefore very general and applies to any $2 \to n$ process with lightlike velocities.

Our argument above clearly depends on the noncollinearity of the three eikonals v_A, v_B, and v_C. When, for example, v_C is taken collinear to v_B, the variables η_i vanish identically or, equivalently, the Jacobian of the transformation vanishes. These arguments therefore do not show the vanishing of diagrams involving the forward scattering of eikonal lines. In fact, the three-gluon diagrams connecting three eikonal lines do *not* vanish when the forward limit is taken before the integrals are performed, at least when the eikonals are taken to have nonzero masses. This calculation is found in Ref. [29]. While superficially similar, however, the meanings of these two calculations are not the same. The factorization properties of forward scattering amplitudes for Wilson lines or partons are quite different than those of fixed-angle scattering amplitudes. For example, unlike the factorization into two incoming and two outgoing jets, as in Eqs. (2.4) and (2.5) above, amplitudes for $2 \to 2$ forward scattering factorize into only two jet functions, each appearing in both initial and final states, along with a soft matrix. The factorization of forward scattering has been discussed for QED in Ref. [31] and, from this point of view, for QCD in Ref. [32], for example.

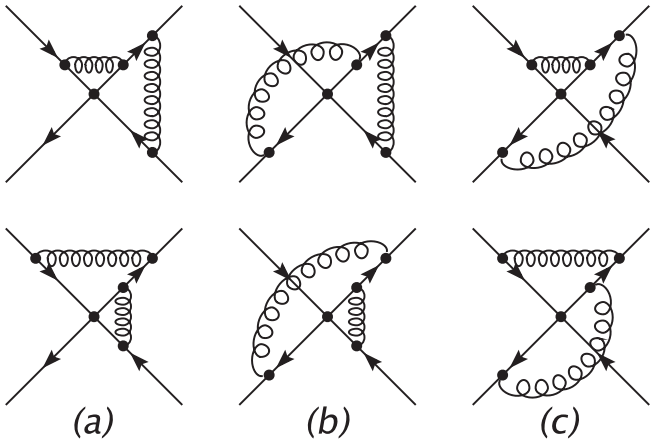

FIG. 4. (a)–(c): Pairs of 3E diagrams.

3. Exponentiation of the remaining 3E diagrams

The only remaining class of diagrams is illustrated by diagram (h) in Fig. 3. Along with its companions found by permuting the eikonal lines, we can refer to these as 3E diagrams, since they are the only nonvanishing diagrams with gluons connected to three eikonal lines. There are 24 such 3E diagrams, 8 of them with s- and t-channel gluon exchanges, 8 of them with s- and u-channel gluons, and finally 8 of them with t- and u-channel gluons. They come in pairs as shown in Fig. 4.

We now show that the analysis of the previous subsection regarding the three-gluon diagrams leads to a very interesting result for the remaining 3E diagrams as well. In this case, the diagrams do not vanish, but reduce to products of one-loop diagrams.[4] They therefore provide no contribution to the two-loop anomalous dimension matrix.

[4]The reduction of a different class of multiloop eikonal diagrams, namely, the 2E diagrams of ladder type, to powers of one-loop diagrams was previously observed in Ref. [33] to hold to all loop orders.

Each such 3E diagram contains one eikonal line with two gluons attached to it, which we label as v_C. The two lines having one gluon attached are labeled v_A and v_B. We will consider a pair of 3E diagrams that are related simply by exchanging the order in which the two gluons attach to v_C, as in Fig. 4(a) for example. The two diagrams have differing color and momentum structures, but we can rewrite their sum as the sum of one term with symmetric color and momentum integrals, plus a second term with antisymmetric color and momentum integrals. In the spirit of the discussion above, we suppress the color matrices held in common and write

$$\mathcal{F}_{ab}(v_A, v_B, v_C) \equiv \mathcal{F}_{ab}^{(\mathrm{sym})}(v_A, v_B, v_C) + \mathcal{F}_{ab}^{(\mathrm{antisym})}(v_A, v_B, v_C), \tag{4.39}$$

where the subscripts a and b refer to the color generators on the v_C eikonal, contracted with generators on the v_A or v_B line, respectively. Consider first the antisymmetric term, which is given by

$$\mathcal{F}_{ab}^{(\mathrm{antisym})}(v_A, v_B, v_C) = \frac{1}{2}(T_b T_a - T_a T_b) \int d^D k_1 d^D k_2 \frac{1}{v_B \cdot k_1 + i\epsilon} \frac{1}{v_A \cdot k_2 + i\epsilon} \frac{1}{k_1^2 + i\epsilon} \frac{1}{k_2^2 + i\epsilon} \frac{1}{v_C \cdot (k_1 + k_2) + i\epsilon} \times \left[\frac{1}{v_C \cdot k_1 + i\epsilon} - \frac{1}{v_C \cdot k_2 + i\epsilon} \right]. \tag{4.40}$$

(In the color-generator notation described in Sec. IV D below, the color operator associated with this antisymmetric term takes the form $[\mathbf{T}_B \cdot \mathbf{T}_C, \mathbf{T}_C \cdot \mathbf{T}_A]$.) The same change of variables, Eq. (4.35), leads to an expression that is again manifestly antisymmetric under the relabeling $\xi_{1,2} \leftrightarrow \eta_{2,1}$, $k_{1,T} \leftrightarrow k_{2,T}$,

$$\begin{aligned}\mathcal{F}_{ab}^{(\mathrm{antisym})}(v_A, v_B, v_C) &= \frac{1}{2}(T_b T_a - T_a T_b) \frac{1}{(v_A \cdot v_C)(v_B \cdot v_C)} \int \prod_{i=1}^{2} d\xi_i d\eta_i d^{D-2} k_{i,T} \frac{1}{2\frac{v_A \cdot v_B}{(v_A \cdot v_C)(v_B \cdot v_C)} \xi_i \eta_i - k_{i,T}^2 + i\epsilon} \\ &\times \frac{1}{\xi_1 + i\epsilon} \frac{1}{\eta_2 + i\epsilon} \frac{1}{\xi_1 + \eta_1 - v_{C,T} \cdot k_{1,T} + i\epsilon} \frac{1}{\xi_2 + \eta_2 - v_{C,T} \cdot k_{2,T} + i\epsilon} \\ &\times \frac{\xi_2 - \xi_1 + \eta_2 - \eta_1 - v_{C,T} \cdot (k_2 - k_1)_T}{\xi_1 + \xi_2 + \eta_1 + \eta_2 - v_{C,T} \cdot (k_1 + k_2)_T + i\epsilon} \\ &= 0. \end{aligned} \tag{4.41}$$

The entire color-antisymmetric part of the infrared region thus vanishes whenever the eikonal approximation is valid, and the cancellation is exact for the eikonal amplitudes we consider here.

Turning to the symmetric term, we need only use the eikonal identity $1/[x(x+y)] + 1/[y(x+y)] = 1/(xy)$ to rewrite it as the product of the two lowest-order single-gluon exchange diagrams,

$$\begin{aligned}\mathcal{F}_{ab}^{(\mathrm{sym})}(v_A, v_B, v_C) &= \frac{1}{2}(T_b T_a + T_a T_b) \\ &\times \int d^D k_1 \frac{1}{v_B \cdot k_1 + i\epsilon} \\ &\times \frac{1}{v_C \cdot k_1 + i\epsilon} \frac{1}{k_1^2 + i\epsilon} \\ &\times \int d^D k_2 \frac{1}{v_A \cdot k_2 + i\epsilon} \\ &\times \frac{1}{v_C \cdot k_2 + i\epsilon} \frac{1}{k_2^2 + i\epsilon}. \end{aligned} \tag{4.42}$$

(In the color-generator notation described in Sec. IV D, the color operator associated with this symmetric term takes the form $\{\mathbf{T}_B \cdot \mathbf{T}_C, \mathbf{T}_C \cdot \mathbf{T}_A\}$.) These diagrams have the correct color and kinematic structure to represent the two-loop terms in the exponentiation of the color-matrix of one-loop infrared poles. They are precisely cancelled in the two-loop soft function by the corresponding products of one-loop counterterms.[5]

We conclude that *the entire two-loop anomalous dimension is due to the 2E diagrams and is given by Eq.* (4.32), in which we may remove the superscript (2E), to obtain

$$\mathbf{\Gamma}_{S_f}^{(2)} = \frac{K}{2} \mathbf{\Gamma}_{S_f}^{(1)}. \tag{4.43}$$

We have thus determined that the two-loop anomalous dimension color-mixing matrix is related to the one-loop matrix by the same factor that relates the one- and two-loop Sudakov anomalous dimensions, $A(\alpha_s)$. Evidently, the next-to-next-to-leading poles in amplitudes with color exchange are generated by the same exponentiation of "webs" as for the elastic form factor [34,35]. Additionally, we note that, in the "bremsstrahlung" or CMW scheme [36], this contribution, along with the corresponding term in the cusp anomalous dimension, is absorbed into a redefinition of the strong coupling, which effectively boosts the strength of parton showering.

[5]Again, as in the discussion of the three-gluon three-eikonal diagrams above, our change of variables does not apply in the case of forward scattering.

C. Expansion of the soft function

To relate the soft anomalous dimension to fixed-order calculations, we expand the resummed soft function, given as a path-ordered exponential in Eq. (2.25), to order $\mathcal{O}(\alpha_s^2)$. The result is

$$\begin{aligned}\mathbf{S}_{\rm f}\left(\frac{Q^2}{\mu^2}=1,\alpha_s(Q^2),\varepsilon\right) &= 1+\frac{1}{2\varepsilon}\left(\frac{\alpha_s}{\pi}\right)\mathbf{\Gamma}^{(1)}_{S_{\rm f}}+\frac{1}{8\varepsilon^2}\left(\frac{\alpha_s}{\pi}\right)^2(\mathbf{\Gamma}^{(1)}_{S_{\rm f}})^2 \\ &\quad -\frac{\beta_0}{16\varepsilon^2}\left(\frac{\alpha_s}{\pi}\right)^2\mathbf{\Gamma}^{(1)}_{S_{\rm f}}+\frac{1}{4\varepsilon}\left(\frac{\alpha_s}{\pi}\right)^2\mathbf{\Gamma}^{(2)}_{S_{\rm f}} \\ &= 1+\frac{1}{2\varepsilon}\left(\frac{\alpha_s}{\pi}\right)\mathbf{\Gamma}^{(1)}_{S_{\rm f}}+\frac{1}{8\varepsilon^2}\left(\frac{\alpha_s}{\pi}\right)^2(\mathbf{\Gamma}^{(1)}_{S_{\rm f}})^2 \\ &\quad -\frac{\beta_0}{16\varepsilon^2}\left(\frac{\alpha_s}{\pi}\right)^2\mathbf{\Gamma}^{(1)}_{S_{\rm f}}+\frac{1}{8\varepsilon}\left(\frac{\alpha_s}{\pi}\right)^2K\mathbf{\Gamma}^{(1)}_{S_{\rm f}},\end{aligned} \tag{4.44}$$

where in the second equality we have used Eq. (4.43) for the two-loop anomalous dimension matrix. Combining this result with the second-order minimal jet function, Eq. (3.7), in the formula for the factorized amplitude, Eq. (3.4), we will derive a result to compare directly with the pole structure of explicit two-loop calculations.

D. Iterative color-matrix form

Given the one- and two-loop soft anomalous dimension matrices (4.23) and (4.43), and the expansion of the quark jet function, as in Eq. (3.7), we can use the factorized amplitude, Eq. (3.4), to calculate all infrared and collinear poles at order α_s^2 for quark-antiquark scattering. The result will be a set of coefficients of the specific basis tensors in color space that we have chosen, Fig. 2. In this basis, we can perform threshold resummation for jet and other cross sections.

To compare to explicit calculations at the two-loop level, however, and to generalize to higher numbers of external partons, it is convenient to make contact with a somewhat different notation, in which the color interactions of soft gluons are represented by a color matrix $\mathbf{T}_i^a$ for the insertion of a gluon on the external line i, with $\mathbf{T}_i^a$ a generator in the color representation of that parton, i, whose color-matrix (rather than generator) indices are summed against those of the lower-order amplitude that is "dressed" by this soft gluon. In the notation of Eq. (2.2) above for the color content of an amplitude, the action of the generators may be made explicit as the action of a vector, with indices in the adjoint representation; for example, for $i = 1$,

$$\begin{aligned}[\mathbf{T}_1^a|\mathcal{M}_{\rm f}\rangle]_{d_1,r_2\ldots} &\equiv \mathcal{M}_L^{[\rm f]}\left(\beta_j,\frac{Q^2}{\mu^2},\alpha_s(\mu^2),\varepsilon\right) \\ &\quad\times\delta_i(T^a)_{d_1r_1}(c_L)_{\{r_1,r_2\ldots\}},\end{aligned} \tag{4.45}$$

where $\delta_i = \pm 1$ absorbs minus signs associated with anti-particles and crossing. In the convention of Ref. [14], $\delta_i = 1$ when i is an eikonal line representing an outgoing quark or gluon, or incoming antiquark; $\delta_i = -1$ for an incoming quark or gluon, or outgoing antiquark. Defined in this way, the vector color-generator matrices obey the fundamental relation $\sum_i \mathbf{T}_i = 0$, which is an expression of gauge invariance. The $\mathbf{T}_i$'s are conventionally normalized to $\mathbf{T}_i \cdot \mathbf{T}_i = C_i$, with $i = q, g$.

A gluon exchanged between two parton lines i and j produces the product $\mathbf{T}_i \cdot \mathbf{T}_j$, which acts on an amplitude in a fashion precisely similar to Eq. (4.45). This notation allows for a convenient iterative expression for color exchange due to soft gluon exchange, without requiring an explicit choice for the color basis.

The color-space notation above may be applied to the computation of the soft function as well as to the amplitude itself. Consider the soft function at a single loop, determined by the one-loop soft anomalous dimension. As we have seen, the latter is built up from the contributions of soft gluon exchanges between pairs of eikonal lines. From each exchange, the contribution to the anomalous dimension is found from Eq. (2.21), where the one-loop single-pole term in $Z_{S_{\rm f}}$ equals the one-loop UV pole term computed from the corresponding diagram.

Each diagrammatic contribution, then, is proportional to a product $\mathbf{T}_i \cdot \mathbf{T}_j$ acting on the lower-order amplitude, multiplied by the result of the eikonal integral. Referring to Fig. 1, the relevant single-pole coefficients are given in Eq. (4.13). The action of $\mathbf{\Gamma}^{(1)}_{S_{\rm f}}$ on the color tensor is the sum of all such terms, with a subtraction for the jet anomalous dimensions; this subtraction is proportional to the identity matrix in color space, as in Eq. (2.23). This gives

$$\begin{aligned}\mathbf{\Gamma}^{(1)}_{S_{\rm f}}\left(\frac{s_{ij}}{\mu^2}\right)|\mathcal{M}_{\rm f}\rangle &= \left[\frac{1}{2}\sum_{i\in{\rm f}}\sum_{j\neq i\in{\rm f}}(\delta_i\mathbf{T}_i\cdot\delta_j\mathbf{T}_j)\left(\frac{-2\varepsilon F^{s.p.}_{s_{ij}}}{(\alpha_s/\pi)}\right)\right. \\ &\quad\left.-\sum_{i\in{\rm f}}\Gamma_2^{[i](1)}\left(\frac{u_0}{v^2}\right)\right]|\mathcal{M}_{\rm f}\rangle \\ &= \left[-\frac{1}{2}\sum_{i\in{\rm f}}\sum_{j\neq i}\mathbf{T}_i\cdot\mathbf{T}_j\ln\left(\frac{-s_{ij}}{Q^2v^2}\right)\right. \\ &\quad\left.-\frac{1}{2}\sum_{i\in{\rm f}}C_i\ln\left(\frac{\mu^2}{Q^2v^2}\right)\right]|\mathcal{M}_{\rm f}\rangle \\ &= \frac{1}{2}\sum_{i\in{\rm f}}\sum_{j\neq i}\mathbf{T}_i\cdot\mathbf{T}_j\ln\left(\frac{\mu^2}{-s_{ij}}\right)|\mathcal{M}_{\rm f}\rangle,\end{aligned} \tag{4.46}$$

where $s_{ij} = (p_i + p_j)^2$, with all momenta defined to flow into (or out of) the amplitude. For the four-parton case above, $s_{12} = s$, $s_{13} = t$, and so forth. The overall $1/2$ compensates for double counting in the sum. To derive the final result, we have used the explicit forms of the δ_i's described above, as well as the identities $\sum_i \mathbf{T}_i = 0$ and $\mathbf{T}_i \cdot \mathbf{T}_i = C_i$ (in the quark scattering case, all $C_i = C_F$). In this notation the color identities enforce the cancellation of the collinear-sensitive $\ln(1/v^2)$ terms.

Identical considerations apply to the two-loop case. The nonvanishing anomalous dimension matrix is again a sum of diagrammatic contributions, corresponding to gluon exchange processes involving two eikonal lines only. As we have seen, these contributions have the same color-generator structure, $\mathbf{T}_i \cdot \mathbf{T}_j$, found at one loop. The 3E diagrams have a more complicated color structure, but they do not contribute to the two-loop soft anomalous dimension matrix.

To be more specific, we saw that diagram (h) in Fig. 3 can be organized into antisymmetric and symmetric color structures, which can be represented as commutators and anticommutators of one-loop color structures, of the form $[\mathbf{T}_i \cdot \mathbf{T}_j, \mathbf{T}_j \cdot \mathbf{T}_k]$ and $\{\mathbf{T}_i \cdot \mathbf{T}_j, \mathbf{T}_j \cdot \mathbf{T}_k\}$. Note that the antisymmetric quantity can be written as

$$[\mathbf{T}_i \cdot \mathbf{T}_j, \mathbf{T}_j \cdot \mathbf{T}_k] = \mathbf{T}_i^a [\mathbf{T}_j^a, \mathbf{T}_j^b] \mathbf{T}_k^b = -i f^{abc} \mathbf{T}_i^a \mathbf{T}_j^b \mathbf{T}_k^c. \tag{4.47}$$

As the final form shows, it is totally antisymmetric under permutations of the three eikonal lines. This is also the form of the color factor for the other type of 3E diagram, the three-gluon diagram (g) in Fig. 3.

As emphasized above, the velocity factors multiplying both commutator and anticommutator structures vanish. (In the case of the anticommutator, the vanishing occurs after adding the one-loop counterterms.) Nevertheless, we display the commutator in Eq. (4.47), because it has occurred in the literature before. We will encounter such terms below in our analysis of explicit two-loop calculations, and show how they are consistent with the specific solution for the soft anomalous dimension, Eq. (4.44), in which this combination of color generators does not appear.

E. Generalizations

The analysis given above applies far beyond the $2 \to 2$ quark-antiquark scattering amplitude. When the soft anomalous dimension is expressed in terms of color generators, as in Eq. (4.46) at one loop, and using this equation and Eq. (4.43) to do so at two loops, the result is slightly less explicit than, say, Eq. (4.23), but it is much more general. When we generalize from quark and antiquark to gluon lines, and when we add more partons in the final state, the only change in our considerations above is to change the color generators $\mathbf{T}_i$, and sum over more variables i and j. The eikonal momentum integrals that give rise to the coefficients of the generators are the same for any choice of parton pairs or triplets.

In these terms, the two-loop results organized in Eqs. (4.43) and (4.46) are not limited to quark-antiquark scattering, but apply to the scattering of any flavor combination. Furthermore, these relations are by no means limited to $2 \to 2$ scattering, and apply to any $2 \to n$ process, as in multijet production. These results, therefore, are a step toward threshold and related resummations in hadronic scattering [3,6] at the level of next-to-next-to-leading logarithm.

At present, however, for the purposes of resummation we must still rely upon the explicit form of the matrix as in Eq. (2.25) to generate the amplitude at arbitrary orders. Anticipating further applications, it will be useful to investigate flexible choices of color basis, perhaps based on the trace notation described, for example, in Ref. [37] (this point was noted in Ref. [6]). We reserve these considerations for future work.

V. SINGLE POLES AT NNLO

In this section, we combine the expansions of the jet and soft functions in the minimal factorized amplitude, Eqs. (3.4) and (3.6), and give an explicit expression for infrared poles to two loops, including single poles. We go on to compare these ''postdictions'' of the two-loop single-pole terms to the results of explicit calculations, and verify that they agree. Traditionally, these results have been presented in a form proposed some time before by Catani [14], and we will briefly review this formalism and relate it to the two-loop expansion of our resummed expressions.

A. Two-loop poles from the factorized amplitude

Here, as above, we adopt the notation $f(\alpha_s) = \sum_n (\alpha_s/\pi)^n f^{(n)}$. In this notation, we can express the Born and one-loop amplitudes for process f in terms of the factorized jet, soft, and hard functions of Eq. (3.6) as

$$|\mathcal{M}_{\rm f}^{(0)}\rangle = |\mathcal{H}_{\rm f}^{(0)}\rangle, \tag{5.1}$$

$$\begin{aligned} |\mathcal{M}_{\rm f}^{(1)}\rangle &= \Big(\sum_{i\in {\rm f}} E^{[i](1)} + \mathbf{S}_{\rm f}^{(1)}\Big)|\mathcal{M}_{\rm f}^{(0)}\rangle + |\mathcal{H}_{\rm f}^{(1)}\rangle \\ &= \Big(-\frac{1}{4}\sum_{i\in {\rm f}}\Big(\frac{1}{2\varepsilon^2}\gamma_K^{[i](1)} + \frac{1}{\varepsilon}\mathcal{G}_0^{[i](1)}\Big) \\ &\quad + \frac{1}{2\varepsilon}\mathbf{\Gamma}_{S_{\rm f}}^{(1)}\Big)|\mathcal{M}_{\rm f}^{(0)}\rangle + |\mathcal{H}_{\rm f}^{(1)}\rangle, \end{aligned} \tag{5.2}$$

where for the jet functions we have used the minimal form (3.3). In the second equality for $|\mathcal{M}_{\rm f}^{(1)}\rangle$, we have used explicit expressions for the jet functions and the soft matrix, the latter from Eq. (4.44). Using these results, we find for the two-loop amplitude,

$$\begin{aligned} |\mathcal{M}_{\rm f}^{(2)}\rangle &= \Big[\frac{1}{2}\Big(\sum_{i\in {\rm f}} E^{[i](1)} + \mathbf{S}_{\rm f}^{(1)}\Big)^2 + \sum_{i\in {\rm f}} E^{[i](2)} + \mathbf{S}_{\rm f}^{(2)} \\ &\quad - \frac{1}{2}(\mathbf{S}_{\rm f}^{(1)})^2\Big]|\mathcal{M}_{\rm f}^{(0)}\rangle \\ &\quad + \Big(\sum_{i\in {\rm f}} E^{[i](1)} + \mathbf{S}_{\rm f}^{(1)}\Big)|\mathcal{H}_{\rm f}^{(1)}\rangle + |\mathcal{H}_{\rm f}^{(2)}\rangle. \end{aligned} \tag{5.3}$$

Now both the $E^{[i](n)}$ and the $\mathbf{S}_{\rm f}^{(n)}$ are given by sums of pure poles in ε. As a result, their squares and products all begin

at $1/\epsilon^2$. At two loops, then, the single-pole terms that multiply the Born amplitude $|\mathcal{M}_{\rm f}^{(0)}\rangle$ in Eq. (5.3) are given entirely by the single poles in $E^{[i](2)}$ and $\mathbf{S}_{\rm f}^{(2)}$. From Eq. (3.3) for the jets, and Eq. (4.44) for the soft matrix, these poles are found from the coefficients of the soft and jet anomalous dimensions,

$$
\begin{aligned}
|\mathcal{M}_{\rm f}^{(2)}\rangle = &\left[\frac{1}{2}\left(\sum_{i\in {\rm f}} E^{[i](1)} + \frac{1}{2\epsilon}\mathbf{\Gamma}_{S_{\rm f}}^{(1)}\right)^2 + \sum_{i\in {\rm f}}\sum_{j=2}^{3} E_j^{[i](2)}\right.\\
&\left. - \frac{\beta_0}{16\epsilon^2}\mathbf{\Gamma}_{S_{\rm f}}^{(1)}\right]|\mathcal{M}_{\rm f}^{(0)}\rangle\\
&+\left[\sum_{i\in {\rm f}} E_1^{[i](2)} + \frac{1}{4\epsilon}\mathbf{\Gamma}_{S_{\rm f}}^{(2)}\right]|\mathcal{M}_{\rm f}^{(0)}\rangle\\
&+\left(\sum_{i\in {\rm f}} E^{[i](1)} + \frac{1}{2\epsilon}\mathbf{\Gamma}_{S_{\rm f}}^{(1)}\right)|\mathcal{H}_{\rm f}^{(1)}\rangle + |\mathcal{H}_{\rm f}^{(2)}\rangle, \qquad (5.4)
\end{aligned}
$$

where we have separated the double- and higher-order pole terms from single-pole terms that multiply the Born amplitude, followed by double and single poles times the one-loop hard scattering, and finally the two-loop hard scattering.

From Eq. (3.9), the two-loop single-pole terms that multiply the Born amplitude $|\mathcal{M}_{\rm f}^{(0)}\rangle$ in Eq. (5.4) are given by

$$
\begin{aligned}
\left[\sum_{i\in {\rm f}} E_1^{[i](2)} + \frac{1}{4\epsilon}\mathbf{\Gamma}_{S_{\rm f}}^{(2)}\right]|\mathcal{M}_{\rm f}^{(0)}\rangle = \frac{1}{\epsilon}\Bigg[&-\frac{\mathcal{G}_0^{[i](2)}}{8} + \frac{\beta_0\mathcal{G}^{[i](1)\prime}(0)}{32}\\
&+\frac{K}{8}\mathbf{\Gamma}_{S_{\rm f}}^{(1)}\Bigg]|\mathcal{M}_{\rm f}^{(0)}\rangle, \qquad (5.5)
\end{aligned}
$$

where we recall the notation of Eq. (3.8) for the coefficients $\mathcal{G}^{[i](n)}(\epsilon)$. Given that the one- and two-loop $\mathcal{G}^{[i](n)}$ have been known for a long time, and that we have just calculated the two-loop soft anomalous dimension matrix, this expression provides an explicit form for the intrinsic two-loop single poles in dimensionally regulated amplitudes.

Note that a redefinition of $\mathbf{S}_{\rm f}^{(1)}$ to include a non-pole term would both change the definition of $|\mathcal{H}_{\rm f}^{(1)}\rangle$ at one loop in Eq. (5.2), and introduce single-pole terms into the $(E^{[i](1)} + \mathbf{S}_{\rm f}^{(1)})^2$ contribution to the two-loop expression, Eq. (5.3). As we shall see below, the Born-times-single-pole terms remain invariant under this shift only if the shift commutes with the $\mathbf{\Gamma}_{S_{\rm f}}^{(1)}$. We therefore need all of the expansion (5.4), in order to make contact with the results of explicit two-loop calculations at the single-pole level.

B. One- and two-loop amplitudes in Catani's notation

To compare to existing calculations, we now review the notation of Ref. [14], in which they are normally presented. We first observe that, in this notation, amplitudes are organized in powers of $(\alpha_s/2\pi)$, rather than (α_s/π). We will distinguish this trivial difference below by a prime in the color states, as $|\mathcal{M}_{\rm f}^{\prime(n)}\rangle = 2^n|\mathcal{M}_{\rm f}^{(n)}\rangle$.

In this formalism, the single- and double-pole structure of one-loop amplitudes is expressed in terms of the color-generator operators introduced above,

$$
\begin{aligned}
\mathbf{I}_{\rm f}^{(1)}(\epsilon) = &\frac{1}{2}\frac{e^{-\epsilon\psi(1)}}{\Gamma(1-\epsilon)}\sum_{i\in {\rm f}}\sum_{j\neq i}(\mathbf{T}_i\cdot\mathbf{T}_j)\left[\frac{1}{\epsilon^2} + \frac{\gamma_i}{\mathbf{T}_i^2}\frac{1}{\epsilon}\right]\\
&\times\left(\frac{\mu^2}{-s_{ij}}\right)^{\epsilon}, \qquad (5.6)
\end{aligned}
$$

with $\psi(1) = -\gamma_E$ the logarithmic derivative of the Gamma function. Here $\gamma_g = \beta_0/2$ and $\mathbf{T}_g^2 = C_A$ for gluons ($i = g$), and $\gamma_i/\mathbf{T}_i^2 = 3/2$ for $i = q$ or $\bar{q}$. The poles of the one-loop amplitude in color-state notation are then represented as

$$
|\mathcal{M}_{\rm f}^{\prime(1)}\rangle = \mathbf{I}_{\rm f}^{(1)}(\epsilon)|\mathcal{M}_{\rm f}^{\prime(0)}\rangle + |\mathcal{M}_{\rm f}^{\prime(1)\,\rm fin}\rangle. \qquad (5.7)
$$

The explicit relation to the resummation formalism at one loop is found by expanding $\mathbf{I}_{\rm f}^{(1)}$ in powers of ϵ,

$$
\begin{aligned}
\mathbf{I}_{\rm f}^{(1)}|\mathcal{M}_{\rm f}^{\prime(0)}\rangle = &\left[2\sum_{i\in {\rm f}} E^{[i](1)}(\epsilon) + \frac{1}{\epsilon}\mathbf{\Gamma}_{S_{\rm f}}^{(1)} + \frac{\zeta(2)}{4}\sum_{i\in {\rm f}}\mathbf{T}_i^2\right.\\
&+\frac{1}{2}\sum_{j\neq i}(\mathbf{T}_i\cdot\mathbf{T}_j)\left(\frac{1}{2}\ln^2\left(\frac{\mu^2}{-s_{ij}}\right)\right.\\
&\left.\left.+\frac{\gamma_i}{\mathbf{T}_i^2}\ln\left(\frac{\mu^2}{-s_{ij}}\right)\right) + \mathcal{O}(\epsilon)\right]|\mathcal{M}_{\rm f}^{\prime(0)}\rangle\\
\equiv &\left[2\sum_{i\in {\rm f}} E^{[i](1)}(\epsilon) + \frac{1}{\epsilon}\mathbf{\Gamma}_{S_{\rm f}}^{(1)} + \mathbf{I}_{\rm f}^{(1)\,\rm fin}\right]|\mathcal{M}_{\rm f}^{\prime(0)}\rangle.
\end{aligned}
\qquad (5.8)
$$

Taking into account the overall factor of 2 from the expansion in $\alpha_s/2\pi$, the pole terms in Eq. (5.7) are thus identical to those in Eq. (5.2). The matrix $\mathbf{I}_{\rm f}^{(1)}$ generates as well explicit μ-dependent finite contributions contained in $\mathbf{I}_{\rm f}^{(1)\,\rm fin}$, which in the minimal factorization are absorbed into the one-loop hard function $|\mathcal{H}_{\rm f}\rangle$. The one-loop infrared finite amplitudes are related by

$$
|\mathcal{H}_{\rm f}^{\prime(1)}\rangle = |\mathcal{M}_{\rm f}^{\prime(1)\,\rm fin}\rangle + \mathbf{I}_{\rm f}^{(1)\,\rm fin}|\mathcal{M}_{\rm f}^{\prime(0)}\rangle. \qquad (5.9)
$$

This is an example of a finite shift of the sort mentioned above, which redefines the finite function at one loop.

At two loops, Ref. [14] predicted the fourth- through second-order poles in terms of the generators $\mathbf{I}_{\rm f}^{(1)}$, and absorbed the then-unknown single-pole contributions in terms of a color operator $\mathbf{H}_{\rm f}^{(2)}$,

$$\mathbf{I}_{\rm f}^{(2)}(\varepsilon) = -\frac{1}{2}\mathbf{I}_{\rm f}^{(1)}(\varepsilon)\left(\mathbf{I}_{\rm f}^{(1)}(\varepsilon) + \frac{\beta_0}{\varepsilon}\right) + \frac{e^{\varepsilon\psi(1)}\Gamma(1-2\varepsilon)}{\Gamma(1-\varepsilon)} \times \left(\frac{\beta_0}{2\varepsilon} + K\right)\mathbf{I}_{\rm f}^{(1)}(2\varepsilon) + \mathbf{H}_{\rm f}^{(2)}(\varepsilon). \tag{5.10}$$

The two-loop amplitude is then organized as

$$|\mathcal{M}_{\rm f}^{\prime(2)}\rangle = \mathbf{I}_{\rm f}^{(2)}(\varepsilon)|\mathcal{M}_{\rm f}^{\prime(0)}\rangle + \mathbf{I}_{\rm f}^{(1)}(\varepsilon)|\mathcal{M}_{\rm f}^{\prime(1)}\rangle + |\mathcal{M}_{\rm f}^{\prime(2)\,\rm fin}\rangle. \tag{5.11}$$

In the intervening years, the color generators $\mathbf{H}_{\rm f}^{(2)}$ have been determined by matching to the single-pole structure of explicit two-loop QCD scattering amplitude calculations, for example, $gg \to gg$, $q\bar{q} \to gg$, $q\bar{q} \to q\bar{q}$, and $e^+e^- \to q\bar{q}g$ [10–12,19,20]. Here we follow Ref. [20] and write

$$\mathbf{H}_{\rm f}^{(2)}(\varepsilon) = \frac{1}{4\varepsilon}\left\{\sum_{i\in \rm f} H_i^{(2)} + \hat{\mathbf{H}}_{\rm f}^{(2)}\right\} + \mathcal{O}(\varepsilon), \tag{5.12}$$

where we split the single-pole factor into a color-diagonal term, which can be represented as a sum of constants $H_i^{(2)}$ for each external parton i, and a matrix $\hat{\mathbf{H}}_{\rm f}^{(2)}$ that includes all color mixing. This matrix can be written as [10–12,19,20]

$$\hat{\mathbf{H}}_{\rm f}^{(2)} = i\sum_{(i,j,k)} f_{a_1a_2a_3}\mathbf{T}_i^{a_1}\mathbf{T}_j^{a_2}\mathbf{T}_k^{a_3} \times \ln\left(\frac{-s_{ij}}{-s_{jk}}\right)\ln\left(\frac{-s_{jk}}{-s_{ki}}\right)\ln\left(\frac{-s_{ki}}{-s_{ij}}\right), \tag{5.13}$$

where the sum is over distinguishable but unordered triplets of external lines (i, j, k). We note the similarity to the color structure from the 3E diagrams, Eq. (4.47). We emphasize that this form has been obtained directly only for processes with at most four partonic legs. In Ref. [20] it was also shown to be consistent with the proper collinear behavior of the $2 \to n$ gluon amplitudes.

It is these expressions that we will compare to the two-loop expansion of the factorized amplitude, Eqs. (5.4) and (5.5). Rather than provide explicit expressions at this point for the constants $H_i^{(2)}$ from Ref. [20], we will derive below expressions relating the constants $H_i^{(2)}$ to the jet anomalous dimensions (in the $\overline{\rm MS}$ scheme). Here we will find useful an identity found in Ref. [38]. The matrix $\hat{\mathbf{H}}_{\rm f}^{(2)}$ in Eq. (5.13) will emerge from our results for the two-loop soft anomalous dimension matrix, plus the effects of a one-loop finite color-mixing term. We now turn to this exercise.

C. $\mathbf{H}^{(2)}$ from the anomalous dimensions

Inserting the definition of $\mathbf{I}_{\rm f}^{(2)}$, Eq. (5.10), into Eq. (5.11) and expanding to the accuracy of ε^0, we readily find

$$|\mathcal{M}_{\rm f}^{\prime(2)}\rangle = \frac{1}{2}(\mathbf{I}_{\rm f}^{(1)}(\varepsilon))^2|\mathcal{M}_{\rm f}^{\prime(0)}\rangle + \left[\frac{\beta_0}{2\varepsilon}(\mathbf{I}_{\rm f}^{(1)}(2\varepsilon) - \mathbf{I}_{\rm f}^{(1)}(\varepsilon)) + \left(K + \frac{3\varepsilon\zeta(2)}{4}\beta_0\right)\mathbf{I}_{\rm f}^{(1)}(2\varepsilon) + \mathbf{H}_{\rm f}^{(2)}(\varepsilon) + \mathcal{O}(\varepsilon^0)\right]|\mathcal{M}_{\rm f}^{\prime(0)}\rangle + \mathbf{I}_{\rm f}^{(1)}(\varepsilon)|\mathcal{M}_{\rm f}^{\prime(1)\,\rm fin}\rangle + |\mathcal{M}_{\rm f}^{\prime(2)\,\rm fin}\rangle. \tag{5.14}$$

We will relate this expression to the single-pole result from the factorized amplitude, Eqs. (5.4) and (5.5).

The single-pole terms in Eq. (5.14) that multiply the Born amplitude come from two sources: the $(\mathbf{I}_{\rm f}^{(1)})^2$ operator on the first line, and the terms in the square brackets on the first and second lines, which also include finite corrections indicated by $+\mathcal{O}(\varepsilon^0)$.

To make contact with the expansion of the resummed amplitude, Eq. (5.4), we first separate the poles in each of the $\mathbf{I}_{\rm f}^{(1)}$ terms, according to Eq. (5.8),

$$|\mathcal{M}_{\rm f}^{\prime(2)}\rangle = \left[\frac{1}{2}\left(2\sum_{i\in \rm f}E^{[i](1)}(\varepsilon) + \frac{1}{\varepsilon}\mathbf{\Gamma}_{S_{\rm f}}^{(1)}\right)^2 + 2\left(\sum_{i\in \rm f}E^{[i](1)}(\varepsilon)\right)\mathbf{I}_{\rm f}^{(1)\,\rm fin}\right]|\mathcal{M}_{\rm f}^{\prime(0)}\rangle + \frac{1}{2}\left[\left(\mathbf{I}_{\rm f}^{(1)\,\rm fin}\frac{1}{\varepsilon}\mathbf{\Gamma}_{S_{\rm f}}^{(1)} + \frac{1}{\varepsilon}\mathbf{\Gamma}_{S_{\rm f}}^{(1)}\mathbf{I}_{\rm f}^{(1)\,\rm fin}\right) + (\mathbf{I}_{\rm f}^{(1)\,\rm fin})^2\right]|\mathcal{M}_{\rm f}^{\prime(0)}\rangle + \left[\frac{\beta_0}{2\varepsilon}\left(2\sum_{i\in \rm f}E^{[i](1)}(2\varepsilon) - 2\sum_{i\in \rm f}E^{[i](1)}(\varepsilon) - \frac{1}{2\varepsilon}\mathbf{\Gamma}_{S_{\rm f}}^{(1)}\right) + \frac{3\zeta(2)\beta_0}{8\varepsilon}\sum_{i\in \rm f}E_2^{[i](1)} + K\left(2\sum_{i\in \rm f}E^{[i](1)}(2\varepsilon) + \frac{1}{2\varepsilon}\mathbf{\Gamma}_{S_{\rm f}}^{(1)}\right) + \mathbf{H}_{\rm f}^{(2)}(\varepsilon) + \mathbf{I}_{\rm f}^{(2)\rm fin}\right]|\mathcal{M}_{\rm f}^{\prime(0)}\rangle + \left[2\sum_{i\in \rm f}E^{[i](1)}(\varepsilon) + \frac{1}{\varepsilon}\mathbf{\Gamma}_{S_{\rm f}}^{(1)} + \mathbf{I}_{\rm f}^{(1)\rm fin}\right]|\mathcal{M}_{\rm f}^{\prime(1)\,\rm fin}\rangle + |\mathcal{M}_{\rm f}^{\prime(2)\,\rm fin}\rangle, \tag{5.15}$$

where in $\mathbf{I}_{\rm f}^{(2)\rm fin}$ we isolate the finite terms from $\mathbf{I}_{\rm f}^{(2)}$ that multiply the Born amplitude. Comparison with Eq. (5.4) requires further that we commute the soft anomalous dimension matrices with poles to the left of the finite amplitudes, and that we also reexpress $|\mathcal{M}^{\prime(1)\rm fin}\rangle$ in terms of $|\mathcal{H}^{\prime(1)}\rangle$ using Eq. (5.9). The first step, in particular, leads to an additional commutator contribution at the level of the single poles times the Born amplitude,

$$|\mathcal{M}_{\rm f}^{\prime(2)}\rangle = \frac{1}{2}\Big(2\sum_{i\in{\rm f}} E^{[i](1)}(\varepsilon) + \frac{1}{\varepsilon}\mathbf{\Gamma}_{S_{\rm f}}^{(1)}\Big)^2 |\mathcal{M}_{\rm f}^{\prime(0)}\rangle + \Big[\frac{\beta_0}{2\varepsilon}\Big(2\sum_{i\in{\rm f}} E^{[i](1)}(2\varepsilon) - 2\sum_{i\in{\rm f}} E^{[i](1)}(\varepsilon) - \frac{1}{2\varepsilon}\mathbf{\Gamma}_{S_{\rm f}}^{(1)}\Big) + K\sum_{i\in{\rm f}}\frac{E_2^{[i](1)}}{2\varepsilon^2}\Big]|\mathcal{M}_{\rm f}^{\prime(0)}\rangle$$
$$+ \Big[\frac{3\zeta(2)\beta_0}{8\varepsilon}\sum_{i\in{\rm f}} E_2^{[i](1)} + K\Big(\sum_{i\in{\rm f}}\frac{E_1^{[i](1)}}{\varepsilon} + \frac{1}{2\varepsilon}\mathbf{\Gamma}_{S_{\rm f}}^{(1)}\Big) + \frac{1}{2\varepsilon}[\mathbf{I}_{\rm f}^{(1)\,\rm fin}, \mathbf{\Gamma}_{S_{\rm f}}^{(1)}] + \mathbf{H}_{\rm f}^{(2)}(\varepsilon)\Big]|\mathcal{M}_{\rm f}^{\prime(0)}\rangle$$
$$+ \Big[2\sum_{i\in{\rm f}} E^{[i](1)}(\varepsilon) + \frac{1}{\varepsilon}\mathbf{\Gamma}_{S_{\rm f}}^{(1)}\Big]|\mathcal{H}_{\rm f}^{\prime(1)}\rangle + |\mathcal{H}_{\rm f}^{\prime(2)}\rangle. \tag{5.16}$$

Here we have organized the expression just as in Eq. (5.4), starting with the square of one-loop pole terms, two-loop second- and third-order poles, and then first-order poles, all times the Born amplitude, followed by poles times the one-loop hard amplitude and finally the two-loop hard part,

$$|\mathcal{H}_{\rm f}^{\prime(2)}\rangle \equiv \Big(\mathbf{I}_{\rm f}^{(2)\,\rm fin} - \frac{1}{2}(\mathbf{I}_{\rm f}^{(1)\,\rm fin})^2\Big)|\mathcal{M}_{\rm f}^{\prime(0)}\rangle + \mathbf{I}_{\rm f}^{(1)\,\rm fin}|\mathcal{H}_{\rm f}^{\prime(1)}\rangle + |\mathcal{M}_{\rm f}^{\prime(2)\,\rm fin}\rangle. \tag{5.17}$$

We are now ready to compare this expression to the two-loop single-pole terms of Eq. (5.5). Higher-order poles can easily be checked in a similar manner [9].

Consider first the matrix parts of Eqs. (5.5) and (5.16). Recalling the factor of 4 associated with changing from the coefficient of $(\alpha_s/\pi)^2$ to $(\alpha_s/2\pi)^2$, we see that the $K\mathbf{\Gamma}_{S_{\rm f}}^{(1)}$ term is identical in the two expressions. Consistency then requires the remarkable result that the commutator of $\mathbf{I}_{\rm f}^{(1)\,\rm fin}$ in Eq. (5.8) with the one-loop soft anomalous dimension in Eq. (4.46) precisely cancel the two-loop $\hat{\mathbf{H}}_{\rm f}^{(2)}$ function as defined in Eq. (5.13),

$$\Big[\mathbf{I}_{\rm f}^{(1)\,\rm fin}, \mathbf{\Gamma}_{S_{\rm f}}^{(1)}\Big] = -\frac{1}{2}\hat{\mathbf{H}}_{\rm f}^{(2)}. \tag{5.18}$$

In fact, a compact calculation, given in Appendix D, shows that Eq. (5.18) indeed holds for the explicit matrix $\hat{\mathbf{H}}_{\rm f}^{(2)}$ given in Eq. (5.13), for arbitrary $2 \to 2$ processes, and also for $2 \to n$ processes where all particles are identical. For those processes with five or more partons for which the quantities $\gamma_i/\mathbf{T}_i^2$ are not all identical, the commutator is more complicated, as can be seen by inspecting Eq. (5.8), and as discussed in Appendix D. Because we know the anomalous dimension matrix for all these processes, however, Eq. (5.18) can be turned around and taken as a definition of the corresponding matrices $\hat{\mathbf{H}}_{\rm f}^{(2)}$. Recently, the soft anomalous dimension matrix $\mathbf{\Gamma}_{S_{\rm f}}^{(2)}$ for $2 \to 2$ processes was computed [18] by making use of just this connection to $\hat{\mathbf{H}}_{\rm f}^{(2)}$, along with the explicit results for $\hat{\mathbf{H}}_{\rm f}^{(2)}$ for quark-quark scattering [10].

The remaining, color-diagonal, single-pole terms in Eq. (5.16) are found using the values of the one-loop quantities $E^{[i](1)}$ given in Eq. (3.9), and the form of $\mathbf{H}_{\rm f}^{(2)}$ given in Eq. (5.12). Then the single poles times Born amplitudes of Eq. (5.16) are given by

$$|\mathcal{M}_{\rm f}^{\prime(2)}\rangle_{\text{single pole} \times \text{Born}} = \frac{1}{\varepsilon}\sum_{i\in{\rm f}}\Big[\frac{H_i^{(2)}}{4} - \frac{3\zeta(2)\beta_0}{32}C_i - \frac{K\mathcal{G}_0^{[i](1)}}{4}\Big]|\mathcal{M}_{\rm f}^{\prime(0)}\rangle + \frac{K}{2\varepsilon}\mathbf{\Gamma}_{S_{\rm f}}^{(1)}|\mathcal{M}_{\rm f}^{\prime(0)}\rangle, \tag{5.19}$$

where we have suppressed dependence that contributes only at the level ε^0. The comparison of Eq. (5.19) with the expansion from the resummed amplitude, Eq. (5.5), is now trivial. We simply appeal to the striking identity noted explicitly by Ravindran, Smith, and van Neerven [38], which in our notation is written as

$$\frac{H_i^{(2)}}{4} - \frac{3\zeta(2)\beta_0}{32}C_i - \frac{K\mathcal{G}_0^{[i](1)}}{4} = 4E_1^{[i](2)}, \tag{5.20}$$

where $E_1^{[i](2)}$ is given in Eq. (3.9). In Ref. [38] this expression was observed to imply a close relationship between the $H_i^{(2)}$ constants and the form factors. We now see that, aside from color mixing, all the single-pole terms are identical to those in the form factors. Indeed, the precise terms relating the $H_i^{(2)}$ to the single-pole residues of the elastic form factor are present simply to cancel a set of "extra" single-pole terms generated from the expansion of $\mathbf{I}_{\rm f}^{(1)}$ in the two-loop amplitude. As in the case of the color-mixing anomalous dimensions, we can also consider Eq. (5.20) as a *definition* of the constants $H_i^{(2)}$.

In summary, we have shown that the full single-pole structure of the two-loop amplitudes can be reconstructed from the same anomalous dimensions that determine the next-to-next-to-leading poles of the factorized jet and soft functions at all orders in pertubation theory. This relation, and the explicit forms of the anomalous dimensions, hold for partonic scattering amplitudes with arbitrary numbers of external lines.

VI. CONCLUSIONS

We have extended the factorization and resummation formalisms for exclusive amplitudes in QCD to next-to-next-to-leading poles in these amplitudes. The same anomalous dimension matrices, calculated here directly for the first time at two loops, control a variety of resummed cross sections at NNLL. These calculations gen-

eralize the determination of the Sudakov anomalous dimensions to nontrivial color mixing.

We verified the formalism and anomalous dimensions by showing that they allow us to reproduce the very nontrivial color and momentum structure of single infrared poles at next-to-next-to-leading order for $2 \to 2$ processes in the literature.

The calculation of the NNLO soft anomalous dimensions opens the door to threshold resummation at next-to-next-to-leading logarithm for multijet cross sections [4,6,7]. Perhaps our most striking result is the discovery that the two-loop soft anomalous dimension matrix is obtained from the one-loop matrix simply by multiplying by $K\alpha_s/(2\pi)$, where K is the constant given in Eq. (4.29). This is exactly the same property obeyed by the scalar Sudakov or "cusp" anomalous dimension.

Aside from its intrinsic interest, this relation will make possible next-to-next-to-leading logarithmic resummation formulas in a closed form, since it will be possible to diagonalize the two-loop anomalous dimension matrix independently of the running of the coupling [34–36], using the same color eigenvectors found at one loop [4,6,7,39,40].

Our analysis applies not only to $2 \to n$ processes relevant to hadronic colliders, but also to the inelastic scattering of a parton by a color-singlet source, as in deep-inelastic scattering, and to the creation of arbitrary numbers of partons from a color-singlet source in leptonic annihilation. It will clearly also be of interest to extend this analysis to massive external lines.

ACKNOWLEDGMENTS

This work was supported in part by the National Science Foundation, Grant No. PHY-0098527 and No. PHY-0354776, and by the Department of Energy under Contract No. DE-AC02-76SF00515. We wish to thank Babis Anastasiou, Carola Berger, Zvi Bern, Stefano Catani, Yuri Dokshitzer, Nigel Glover, David Kosower, Hans Kühn, Alexander Penin, Jack Smith, and Werner Vogelsang for very helpful conversations. L. D. wishes to thank the Kavli Institute for Theoretical Physics and the Aspen Center for Physics for support during a portion of this work, and G. S. thanks the Stanford Linear Accelerator Center for hospitality. The figures were generated using JAXODRAW [42], based on AXODRAW [43].

APPENDIX A: ANOMALOUS DIMENSIONS

In this appendix, we provide the low-order anomalous dimensions entering the jet function, as defined in Eqs. (2.7) and (3.7). We give the nth-order coefficients $\gamma_K^{[i](n)}$, $\mathcal{K}^{[i](n)}$, and $\mathcal{G}^{[i](n)}$ in an expansion in powers of $\alpha_s(\mu^2)/\pi$,

$$
\begin{aligned}
&\gamma_K^{[i](1)} = 2C_i, \qquad \gamma_K^{[i](2)} = C_i K = C_i\left[C_A\left(\frac{67}{18} - \zeta(2)\right) - \frac{10}{9}T_F n_F\right], \qquad \mathcal{K}^{[i](1)} = \frac{1}{2\varepsilon}\gamma_K^{[i](1)},\\
&\mathcal{K}^{[i](2)} = \frac{1}{4\varepsilon}\gamma_K^{[i](2)} - \frac{\beta_0}{16\varepsilon^2}\gamma_K^{[i](1)}, \qquad \mathcal{G}^{[q](1)} = \frac{3}{2}C_F + \varepsilon\frac{C_F}{2}(8 - \zeta(2)) + \mathcal{O}(\varepsilon^2),\\
&\mathcal{G}_0^{[q](2)} = 3C_F^2\left[\frac{1}{16} - \frac{1}{2}\zeta(2) + \zeta(3)\right] + \frac{1}{4}C_A C_F\left[\frac{2545}{108} + \frac{11}{3}\zeta(2) - 13\zeta(3)\right] - C_F T_F n_F\left[\frac{209}{108} + \frac{1}{3}\zeta(2)\right],\\
&\mathcal{G}^{[g](1)} = \frac{\beta_0}{2} - \varepsilon\frac{C_A}{2}\zeta(2) + \mathcal{O}(\varepsilon^2),\\
&\mathcal{G}_0^{[g](2)} = C_A^2\left[\frac{10}{27} - \frac{11}{12}\zeta(2) - \frac{1}{4}\zeta(3)\right] + C_A T_F n_F\left[\frac{13}{27} + \frac{1}{3}\zeta(2)\right] + \frac{1}{2}C_F T_F n_F + \frac{\beta_1}{4},
\end{aligned}
\tag{A1}
$$

where $C_q = C_F$, $C_g = C_A$, and

$$
\beta_1 = \frac{34}{3}C_A^2 - 4C_F T_F n_F - \frac{20}{3}C_A T_F n_F. \tag{A2}
$$

The results for $\mathcal{G}^{[i](n)}$ were obtained from Ref. [27], which also contains results through three loops. We shift the gluonic expressions by terms proportional to β-function coefficients, which take into account the effects of renormalizing the operator $G^a_{\mu\nu}G^{a\mu\nu}$, as explained in Ref. [38]. Because we only quote results through two-loop order, some of the results for $\mathcal{G}^{[i](n)}$ could also have been extracted from the two-loop quark electromagnetic form factor [25] and from the $gg \to$ Higgs boson amplitude [26].

APPENDIX B: ONE-LOOP VELOCITY FACTORS

1. Basic integrals

Consider the one-loop t-channel diagram shown in Fig. 1(a). The velocity factor is given by

$$
\begin{aligned}
F_t &= (ig\mu^\varepsilon)^2(v_1 \cdot v_3)\int_0^\infty d\alpha \int_0^\infty d\beta\, D(v_3\alpha + v_1\beta)\\
&= (ig\mu^\varepsilon)^2\frac{1}{4\pi^{2-\varepsilon}}\Gamma(1-\varepsilon)(v_1 \cdot v_3)\\
&\quad \times \int_0^\infty d\alpha \int_0^\infty d\beta \frac{1}{[(v_3\alpha + v_1\beta)^2]^{1-\varepsilon}}.
\end{aligned}
\tag{B1}
$$

We will use the following change of variables:

$$\alpha + \beta \equiv \eta, \qquad \alpha \equiv z\eta, \tag{B2}$$

with Jacobian η. For infrared regularization we impose $\alpha < \frac{1}{\lambda} \Leftrightarrow \eta < \frac{1}{\lambda z}$.[6] Also note that $0 < z < 1$. In terms of the new variables, we have

$$\begin{aligned} F_t &= (ig\mu^\varepsilon)^2 \frac{1}{4\pi^{2-\varepsilon}} \Gamma(1-\varepsilon)(v_1 \cdot v_3) \\ &\quad \times \int_0^1 dz \int_0^{1/\lambda z} d\eta \eta^{2\varepsilon-1} \frac{1}{[(v_3 z + v_1(1-z))^2]^{1-\varepsilon}} \\ &= (ig\mu^\varepsilon)^2 \frac{1}{4\pi^{2-\varepsilon}} \Gamma(1-\varepsilon)(v_1 \cdot v_3) \frac{1}{2\varepsilon} \frac{1}{\lambda^{2\varepsilon}} \\ &\quad \times \int_0^\infty dz' \frac{1}{[(v_3 + v_1 z'))^2]^{1-\varepsilon}}, \end{aligned} \tag{B3}$$

with $z' \equiv \frac{1}{z} - 1$. From the expansion of the above expression, the single-pole term and the finite part of the one-loop diagram are given by

$$\begin{aligned} F_t &= -\left(\frac{\alpha_s}{\pi}\right)(v_1 \cdot v_3)\left\{\frac{1}{2\varepsilon} I_1(v_1, v_3) + \frac{1}{2} I_m(v_1, v_3) \right. \\ &\quad \left. + \frac{1}{2}\left[\ln\left(\frac{\mu^2}{\lambda^2}\right) + \ln(\pi e^{\gamma_E})\right] I_1(v_1, v_3)\right\}, \end{aligned} \tag{B4}$$

where we have defined the following integrals:

$$\begin{aligned} I_1(v_1, v_3) &\equiv \int_0^1 dz \frac{1}{(v_3 z + v_1 \bar{z})^2} = \int_0^\infty dz' \frac{1}{(v_3 + v_1 z')^2}, \\ I_m(v_1, v_3) &\equiv \int_0^\infty dz' \frac{\ln(v_3 + v_1 z')^2}{(v_3 + v_1 z')^2}, \end{aligned} \tag{B5}$$

with $\bar{z} \equiv 1 - z$.

2. Evaluation of I_1 and I_m

We are evaluating eikonal diagrams derived from external Wilson lines. By looking at the usual momentum-space expressions for the amplitudes, one can easily see that all these diagrams are scale independent in the eikonal velocities v_i. With this property in mind we can simplify the evaluations of the integrals by choosing $v_i^2 = 1$ without loss of generality.

In order to evaluate $I_1(v_1, v_3)$ we use the following change of variable [28]:

$$e^{2\psi} \equiv \frac{\sqrt{v_3^2} z + \sqrt{v_1^2}\bar{z} e^{\gamma_{13}}}{\sqrt{v_3^2} z + \sqrt{v_1^2}\bar{z} e^{-\gamma_{13}}}, \tag{B6}$$

which gives

$$\frac{d\psi}{dz} = -\frac{1}{2} \frac{\sqrt{v_1^2 v_3^2}(e^{\gamma_{13}} - e^{-\gamma_{13}})}{(v_3 z + v_1 \bar{z})^2}. \tag{B7}$$

From this change of variable it is very easy to see that

$$\int_0^{\gamma_{13}} d\psi = \sqrt{v_1^2 v_3^2} \sinh\gamma_{13} \int_0^1 dz \frac{1}{(v_3 z + v_1 \bar{z})^2}. \tag{B8}$$

Therefore, we get

$$I_1(v_1, v_3) = \frac{1}{\sqrt{v_1^2 v_3^2} \sinh\gamma_{13}} \gamma_{13}. \tag{B9}$$

Note that

$$I_1(v_1, -v_3) = \frac{1}{\sqrt{v_1^2 v_3^2} \sinh\gamma_{13}} (i\pi - \gamma_{13}), \tag{B10}$$

by analytic continuation.

With $v_i^2 = 1$, I_m can be written as

$$\begin{aligned} I_m(v_1, v_3) &= \int_0^\infty dy \frac{1}{(y + e^{-\gamma_{13}})(y + e^{\gamma_{13}})} \ln[(y + e^{-\gamma_{13}})(y + e^{\gamma_{13}})] \\ &= \frac{1}{2\sinh\gamma_{13}} \int_0^\infty dy \left\{\frac{\ln[(y + e^{-\gamma_{13}})(y + e^{\gamma_{13}})]}{y + e^{-\gamma_{13}}} - \frac{\ln[(y + e^{-\gamma_{13}})(y + e^{\gamma_{13}})]}{y + e^{\gamma_{13}}}\right\} \\ &= \frac{1}{2\sinh\gamma_{13}} \int_0^\infty dy \left\{\frac{\ln(y + e^{-\gamma_{13}})}{y + e^{-\gamma_{13}}} + \frac{\ln(y + e^{\gamma_{13}})}{y + e^{-\gamma_{13}}} - \frac{\ln(y + e^{-\gamma_{13}})}{y + e^{\gamma_{13}}} - \frac{\ln(y + e^{\gamma_{13}})}{y + e^{\gamma_{13}}}\right\}. \end{aligned} \tag{B11}$$

It is easy to verify that the first and last terms in the right-hand side of the final expression cancel, for example by changing variables to $u = y + e^{-\gamma_{13}}$ in the first term and $u = y + e^{\gamma_{13}}$ in the last. This leaves us with

$$\begin{aligned} I_m(v_1, v_3) &= \frac{1}{2\sinh\gamma_{13}} \int_0^\infty dy \left\{\frac{\ln(y + e^{\gamma_{13}})}{y + e^{-\gamma_{13}}} \right. \\ &\quad \left. - \frac{\ln(y + e^{-\gamma_{13}})}{y + e^{\gamma_{13}}}\right\}. \end{aligned} \tag{B12}$$

In the high-energy limit $\gamma \gg 1$, where $e^\gamma \gg e^{-\gamma}$, one easily finds

$$\begin{aligned} I_m(v_1, v_3) &= \frac{1}{2\sinh\gamma_{13}}[-\mathrm{Li}_2(-e^{2\gamma_{13}}) + \mathrm{Li}_2(1) \\ &\quad + \mathcal{O}(e^{-\gamma_{13}})] \\ &= \frac{1}{\sinh\gamma_{13}}\left[\frac{\pi^2}{6} + \gamma_{13}^2 + \mathcal{O}(e^{-\gamma_{13}})\right]. \end{aligned} \tag{B13}$$

Following the same steps, one also gets

[6] For these one-loop diagrams there is one overall IR divergence since all the collinear singularities factorize. Therefore, it is sufficient to restrict only one of the gluon attachments.

$$I_m(v_1, -v_3) = -\frac{1}{\sinh\gamma_{13}}\left[\frac{\pi^2}{6} + \gamma_{13}^2 + \mathcal{O}(e^{-\gamma_{13}})\right]. \tag{B14}$$

APPENDIX C: VELOCITY FACTORS FOR 2E DIAGRAMS

We begin our analysis of the 2E diagrams with the diagram that has a three-gluon vertex, Fig. 3(f). We follow Refs. [28,41] and write the three-gluon vertex as

$$V_{\mu\nu\rho}(k, l, -k-l) = \bar{V}_{\mu\nu\rho}(k, l) + D_{\mu\nu\rho}(k, l), \tag{C1}$$

where

$$\begin{aligned}\bar{V}_{\mu\nu\rho}(k, l) &= (2l + k)_\mu g_{\nu\rho} + 2k_\rho g_{\mu\nu} - 2k_\nu g_{\mu\rho},\\ D_{\mu\nu\rho}(k, l) &= -l_\nu g_{\mu\rho} - (k + l)_\rho g_{\mu\nu},\end{aligned} \tag{C2}$$

and where k and l are the loop momenta. Indices ν and ρ attach to the v_3 line. The diagram resulting from $\bar{V}_{\mu\nu\rho}$ is proportional to v_3^2 before integration. We also note that the contributions of Figs. 3(d) and 3(e) are entirely proportional to v_3^2 before integration, since a single gluon propagator attaches twice to the same eikonal line. These v_3^2 contributions turn out to cancel each other in the high-energy limit. We give the result for the $\bar{V}_{\mu\nu\rho}$ contribution below.

The contribution resulting from the $D_{\mu\nu\rho}$ piece for the diagram of Fig. 3(f) is given by

$$\begin{aligned}W_{2E,3g-D}(v_1, v_3) = -(g\mu^\varepsilon)^4 d_{JI}^{[I]}\frac{C_A}{2}\int\frac{d^Dk}{(2\pi)^D}\frac{d^Dl}{(2\pi)^D}\frac{1}{k^2}\frac{1}{l^2}\\ \times\frac{1}{(k+l)^2}\left[\frac{2v_3\cdot v_1}{(v_1\cdot k)(v_3\cdot k)} + \frac{v_3\cdot v_1}{(v_1\cdot k)(v_3\cdot l)}\right],\end{aligned} \tag{C3}$$

where we have suppressed factors of $i\epsilon$ in the denominators. One can evaluate the above expression in either momentum or configuration space. We will not review the derivation of the following result [28],

$$W_{2E,3g-D}^{s.p.} = \left(\frac{\alpha_s}{\pi}\right)^2 d_{JI}^{[I]}\frac{C_A}{2}\left\{\gamma_{13}\coth\gamma_{13}\left(-\frac{1}{4\varepsilon} + \frac{1}{16\varepsilon}\zeta(2)\right) + \frac{1}{8\varepsilon}I_2(\gamma_{13})\right\}, \tag{C4}$$

where

$$I_2(\gamma_{13}) \equiv \sinh 2\gamma_{13}\int_0^{\gamma_{13}} d\psi\frac{\psi\coth\psi}{\sinh^2\gamma_{13} - \sinh^2\psi} \times \ln\left(\frac{\sinh\gamma_{13}}{\sinh\psi}\right). \tag{C5}$$

We analyze I_2 in order to get the high-energy behavior of this amplitude. We start by writing I_2 as

$$I_2 = I_{cth-1} + I_1, \tag{C6}$$

where

$$\begin{aligned}I_{cth-1} &= \int_0^{\gamma_{13}} d\psi\left[\frac{\sinh 2\gamma_{13}}{\sinh^2\gamma_{13} - \sinh^2\psi}\ln\left(\frac{\sinh\gamma_{13}}{\sinh\psi}\right)\right]\\ &\quad\times\psi(\coth\psi - 1)\\ &= 2\int_0^{\gamma_{13}} d\psi\left[\frac{\sinh 2\gamma_{13}}{\sinh^2\gamma_{13} - \sinh^2\psi}\ln\left(\frac{\sinh\gamma_{13}}{\sinh\psi}\right)\right]\\ &\quad\times\psi\frac{e^{-2\psi}}{1 - e^{-2\psi}},\end{aligned} \tag{C7}$$

and where

$$I_1 = \int_0^{\gamma_{13}} d\psi\left[\frac{\sinh 2\gamma_{13}}{\sinh^2\gamma_{13} - \sinh^2\psi}\ln\left(\frac{\sinh\gamma_{13}}{\sinh\psi}\right)\right]\psi. \tag{C8}$$

Note that I_{cth-1} is exponentially suppressed in ψ when $\psi \sim \gamma_{13}$. However, for small ψ the factor $\frac{\sinh 2\gamma_{13}}{\sinh^2\gamma_{13} - \sinh^2\psi} = 2 + \mathcal{O}(e^{-\gamma_{13}})$. Therefore we can rewrite I_{cth-1} as

$$\begin{aligned}I_{cth-1} &= \int_0^\infty d\psi\left[2\ln\left(\frac{2\sinh\gamma_{13}}{2\sinh\psi}\right)\right]\psi(\coth\psi - 1) + \mathcal{O}(e^{-\gamma_{13}})\\ &= 2\left[\gamma_{13}\int_0^\infty d\psi\psi(\coth\psi - 1) - \int_0^\infty d\psi\psi^2(\coth\psi - 1)\right.\\ &\quad\left. - \int_0^\infty d\psi\psi\ln(1 - e^{-2\psi})(\coth\psi - 1)\right]\\ &\equiv 2(k_1\gamma_{13} + k_2 + k_3).\end{aligned} \tag{C9}$$

We evaluate k_1, k_2, and k_3 separately, starting with

$$\begin{aligned}k_1 &= \int_0^\infty d\psi\psi(\coth\psi - 1) = 2\int_0^\infty d\psi\psi\frac{e^{-2\psi}}{1 - e^{-2\psi}}\\ &= 2\sum_{n=0}^\infty\int_0^\infty d\psi\psi e^{-2(n+1)\psi} = \frac{1}{2}\zeta(2).\end{aligned} \tag{C10}$$

We evaluate k_2 and k_3 by using the same expansion with answers

$$k_2 = -\int_0^\infty d\psi\psi^2(\coth\psi - 1) = -\frac{1}{2}\zeta(3), \tag{C11}$$

and finally

$$k_3 = -\int_0^\infty d\psi\psi\ln(1 - e^{-2\psi})(\coth\psi - 1) = \frac{1}{2}\zeta(3). \tag{C12}$$

Combining these results one finds

$$I_{cth-1} = \zeta(2)\gamma_{13}. \tag{C13}$$

Now let us look at the remaining integral in Eq. (C6), I_1. After some trivial algebra one can rewrite I_1 as

$$I_1 = k_4 + k_5, \tag{C14}$$

where

$$k_4 = 2\int_0^{\gamma_{13}} d\psi\psi(\gamma_{13}-\psi)\frac{1}{(1-e^{-(\gamma_{13}-\psi)})(1+e^{-(\gamma_{13}-\psi)})} + \mathcal{O}(e^{-2\gamma_{13}})$$
$$= 2\gamma_{13}\int_0^{\gamma_{13}} d\lambda\lambda\sum_{n=0}^{\infty} e^{-2n\lambda} - 2\int_0^{\gamma_{13}} d\lambda\lambda^2\sum_{n=0}^{\infty} e^{-2n\lambda} + \mathcal{O}(e^{-2\gamma_{13}}), \quad \text{(C15)}$$

with $\lambda \equiv \gamma_{13}-\psi$, from which

$$k_4 = 2\left[\frac{\gamma_{13}^3}{6} + \gamma_{13}\frac{\zeta(2)}{4} - \frac{\zeta(3)}{4}\right]. \quad \text{(C16)}$$

Finally k_5 is given by

$$k_5 = -2\int_0^{\infty} d\psi\psi\ln(1-e^{-2\psi}) = \frac{\zeta(3)}{2}, \quad \text{(C17)}$$

by using the same kind of manipulations. Combining the above results one finds

$$I_1 = \frac{\gamma_{13}^3}{3} + \frac{\zeta(2)}{2}\gamma_{13}. \quad \text{(C18)}$$

Using Eqs. (C13) and (C18), one finds, for the asymptotic behavior of I_2,

$$I_2(v_1,v_3) = \frac{\gamma_{13}^3}{3} + \frac{3\zeta(2)}{2}\gamma_{13} + \mathcal{O}(e^{-\gamma_{13}}). \quad \text{(C19)}$$

By using this result in the expression for the single-pole term, $W^{s.p.}_{2E,3g-D}$, we find

$$W^{s.p.}_{2E,3g-D} = \left(\frac{\alpha_s}{\pi}\right)^2 d_{JI}^{[t]} C_A \frac{1}{2}\left\{-\frac{1}{4\varepsilon}\gamma_{13} + \frac{1}{16\varepsilon}\left[\frac{2}{3}\gamma_{13}^3 + 4\zeta(2)\gamma_{13}\right]\right\} + \mathcal{O}(e^{-\gamma_{13}})$$
$$= -\left(\frac{\alpha_s}{\pi}\right)^2 d_{JI}^{[t]}\frac{C_A}{2}\frac{1}{4\varepsilon}\left[-\frac{\gamma_{13}^3}{6} + (1-\zeta(2))\gamma_{13}\right] + \mathcal{O}(e^{-\gamma_{13}}). \quad \text{(C20)}$$

The contribution of the $\bar{V}_{\mu\nu\rho}$ piece to the diagram in Fig. 3(f) is given by [28]

$$W^{s.p.}_{2E,3g-\bar{V}} = -\left(\frac{\alpha_s}{\pi}\right)^2 d_{JI}^{[t]}\frac{C_A}{2}\frac{1}{4\varepsilon}\left[-\gamma_{13} + \frac{\zeta(2)}{4} + \frac{1}{2}I_3(\gamma_{13}) + \mathcal{O}(e^{-\gamma_{13}})\right], \quad \text{(C21)}$$

where

$$I_3(\gamma_{13}) \equiv \sinh(2\gamma_{13})\int_0^{\gamma_{13}} d\psi\frac{1}{\sinh^2\gamma_{13}-\sinh^2\psi} \times \ln\left(\frac{\sinh\gamma_{13}}{\sinh\psi}\right). \quad \text{(C22)}$$

One can analyze the high-energy asymptotics of I_3 in a similar way as above, with the result

$$I_3(\gamma_{13}) = \gamma_{13}^2 + \frac{3\zeta(2)}{2} + \mathcal{O}(e^{-\gamma_{13}}). \quad \text{(C23)}$$

Combining Eqs. (C20), (C21), and (C23), and letting $\gamma_{13} = T$, we find

$$W^{s.p.}_{2E,3g} = -\left(\frac{\alpha_s}{\pi}\right)^2 d_{JI}^{[t]}\frac{C_A}{2}\frac{1}{4\varepsilon}\left\{\left[-\frac{T^3}{6} + (1-\zeta(2))T\right] + \left[\frac{T^2}{2} - T + \zeta(2)\right]\right\} + \mathcal{O}(e^{-\gamma_{13}}), \quad \text{(C24)}$$

which is the result given in Eq. (4.26).

The amplitudes for diagrams (d) and (e) of Fig. 3 are given in Ref. [29] and the high-energy asymptotics is obtained with a similar analysis. The results are given in Eq. (4.27). As mentioned above, these contributions cancel the $\bar{V}_{\mu\nu\rho}$ contribution from diagram (f), which is enclosed by the second set of brackets in Eq. (C24).

Finally, let us look at the crossed-ladder diagram in Fig. 3(b). The velocity factor in configuration space is given by

$$F_{CL,t}(v_1,v_3) = (ig\mu^{\varepsilon})^4(v_1\cdot v_3)^2\int_0^{\infty} d\alpha_1\int_0^{\alpha_1} d\alpha_2 \times\int_0^{\infty} d\beta_1\int_0^{\beta_1} d\beta_2 D(v_1\alpha_1+v_3\beta_2) \times D(v_1\alpha_2+v_3\beta_1). \quad \text{(C25)}$$

It is not difficult to show that the single-pole part of the crossed-ladder velocity factor is precisely the negative of that for the uncrossed-ladder diagram in Fig. 3(a). Therefore, in the combination of the two diagrams, the single-pole part of Eq. (C25) is multiplied by the difference of the respective color factors. Although the individual color factors are not proportional to the one-loop factor $d_{JI}^{[t]}$, their difference evaluates to $d_{JI}^{[t]}C_A/2$. The following result for the combination of diagrams (a) and (b) can also be found in Ref. [28],[7]

$$W^{s.p.}_{CL+L,t} = -\left(\frac{\alpha_s}{\pi}\right)^2 d_{JI}^{[t]}\frac{C_A}{2}\frac{1}{2\varepsilon}\coth^2\gamma_{13}\, I_4(v_1,v_3), \quad \text{(C26)}$$

where we define

$$I_4(v_1,v_3) \equiv \int_0^{\gamma_{13}} d\psi\psi(\gamma_{13}-\psi)\coth\psi. \quad \text{(C27)}$$

One can investigate the asymptotic behavior of I_4 in a way similar to that presented for the three-gluon vertex diagram in Fig. 3(f). One obtains the result

$$I_4(v_1,v_3) = \frac{\gamma_{13}^3}{6} + \frac{\zeta(2)}{2}\gamma_{13} - \frac{\zeta(3)}{2} + \mathcal{O}(e^{-\gamma_{13}}). \quad \text{(C28)}$$

By using the above relation in Eq. (C26), we find

$$W^{s.p.}_{CL+L,t} = -\left(\frac{\alpha_s}{\pi}\right)^2 d_{JI}^{[t]}\frac{C_A}{2}\frac{1}{2\varepsilon}\left(\frac{\gamma_{13}^3}{6} + \frac{\zeta(2)}{2}\gamma_{13} - \frac{\zeta(3)}{2}\right) + \mathcal{O}(e^{-\gamma_{13}}). \quad \text{(C29)}$$

[7]Needless to say, we can evaluate the integrals in momentum space and get the same result.

Letting $\gamma_{13} = T$, this is the result given in Eq. (4.25), along with the result for diagram (c) [28].

APPENDIX D: THE COMMUTATOR OF $\mathbf{I}_{\mathrm{f}}^{(1)\,\mathrm{fin}}$ AND $\mathbf{\Gamma}_{S_{\mathrm{f}}}^{(1)}$

The task of this appendix is to evaluate the commutator $[\mathbf{I}_{\mathrm{f}}^{(1)\mathrm{fin}}, \mathbf{\Gamma}_{S_{\mathrm{f}}}^{(1)}]$ appearing on the left-hand side of Eq. (5.18). Note that the pole parts of $\mathbf{I}_{\mathrm{f}}^{(1)}$ can be identified with $\mathbf{\Gamma}_{S_{\mathrm{f}}}^{(1)}$, via Eq. (5.8). Writing out the $\mathcal{O}(\varepsilon^0)$ parts of $\mathbf{I}_{\mathrm{f}}^{(1)\,\mathrm{fin}}$ with nontrivial color structure, the commutator of the finite and pole parts of $\mathbf{I}_{\mathrm{f}}^{(1)}$ becomes

$$\begin{aligned}\left[\mathbf{I}_{\mathrm{f}}^{(1)\,\mathrm{fin}}, \mathbf{\Gamma}_{S_{\mathrm{f}}}^{(1)}\right] &= \frac{1}{4}\Bigg[\sum_k \sum_{l\neq k} (\mathbf{T}_k \cdot \mathbf{T}_l)\left(\frac{1}{2}\ln^2\left(\frac{\mu^2}{-s_{kl}}\right)\right. \\ &\qquad \left. + \frac{\gamma_k}{\mathbf{T}_k^2}\ln\left(\frac{\mu^2}{-s_{kl}}\right)\right), \sum_i \sum_{j\neq i} (\mathbf{T}_i \cdot \mathbf{T}_j)\ln\left(\frac{\mu^2}{-s_{ij}}\right)\Bigg] \\ &= \mathcal{C}_{3,\mathrm{f}} + \mathcal{C}_{2,\mathrm{f}}, \end{aligned} \tag{D1}$$

where in the second equality we introduce notation to separate the terms with three logarithms ($\mathcal{C}_{3,\mathrm{f}}$) from those with two ($\mathcal{C}_{2,\mathrm{f}}$).

In the case where all external lines are gluons, or all are quarks and/or antiquarks, all the ratios $\gamma_k/\mathbf{T}_k^2$ in the left-hand side of the commutator are equal. This term is then proportional to $\mathbf{\Gamma}_{S_{\mathrm{f}}}^{(1)}$, and $\mathcal{C}_{2,\mathrm{f}}$ vanishes. This argument does not apply, of course, to mixed processes, such as $q\bar{q} \to gg$. For the latter case, however, and for any other $2 \to 2$ process, we may use the color conservation identity $\sum_k \mathbf{T}_k = 0$ and the simplicity of the kinematics to show that $\mathcal{C}_{2,\mathrm{f}}$ vanishes. The argument is simple, and may be given for the case $q\bar{q} \to gg$ without loss of generality. In this case, we may take $k = 1, 2$ in Eq. (D1) to correspond to the incoming quark and antiquark, and we consider just these terms in the double-logarithmic part of the commutator in Eq. (D1). We focus first on the terms with prefactor $\gamma_q/\mathbf{T}_q^2 = 3/2$. (The same argument applies to the remaining terms, with prefactor $\gamma_g/\mathbf{T}_g^2$.) These terms are proportional to

$$\left[\sum_{k=1}^{2}\sum_{l\neq k} \mathbf{T}_k \cdot \mathbf{T}_l \ln\left(\frac{\mu^2}{-s_{kl}}\right), \sum_{i=1}^{4}\sum_{j\neq i} \mathbf{T}_i \cdot \mathbf{T}_j \ln\left(\frac{\mu^2}{-s_{ij}}\right)\right]. \tag{D2}$$

This commutator would vanish if the sum over index k were extended to $k = 3$ and 4. But this can by done by observing that $\sum_k \mathbf{T}_k = 0$ implies, for example,

$$\mathbf{T}_1 \cdot \mathbf{T}_2 = \mathbf{T}_3 \cdot \mathbf{T}_4 + \tfrac{1}{2}(T_3^2 + T_4^2 - T_1^2 - T_2^2), \tag{D3}$$

where the squared terms commute with all combinations of generators. At the same time, we have $s_{12} = s_{34}$. As a result, in the left-hand term of the commutator (D2), we may make the replacement

$$\mathbf{T}_1 \cdot \mathbf{T}_2 \ln\left(\frac{\mu^2}{-s_{12}}\right) \to \mathbf{T}_3 \cdot \mathbf{T}_4 \ln\left(\frac{\mu^2}{-s_{34}}\right). \tag{D4}$$

Analogous reasoning for each of the terms in the sum over k and l in Eq. (D2) shows that for $2 \to 2$ scattering the sum of the missing terms with $k = 3$, 4 is identical in the commutator to the sum from $k = 1$, 2. Inserting the missing terms, at the price of an overall factor of $1/2$, the two entries of the commutator become identical and it vanishes. This argument, of course, is heavily dependent on the specifics of $2 \to 2$ scattering. We know of no general argument that would eliminate all double-logarithmic terms in the commutator in $2 \to n$ processes; indeed such terms are generically present.

We now consider the triple-logarithmic terms in Eq. (D1),

$$\begin{aligned}\mathcal{C}_{3,\mathrm{f}} &= \frac{1}{8}\Bigg[\sum_k \sum_{l\neq k} \mathbf{T}_k \cdot \mathbf{T}_l, \sum_i \sum_{j\neq i} \mathbf{T}_i \cdot \mathbf{T}_j\Bigg] b_{kl} a_{ij} \\ &= \frac{1}{2}\sum_{i\neq j\neq k} [\mathbf{T}_k \cdot \mathbf{T}_j, \mathbf{T}_j \cdot \mathbf{T}_i]\, b_{kj} a_{ij} \\ &= \frac{1}{2}\sum_{i\neq j\neq k} i f_{a_1 a_2 a_3} \mathbf{T}_k^{a_1} \mathbf{T}_j^{a_3} \mathbf{T}_i^{a_2} b_{kj} a_{ij}, \end{aligned} \tag{D5}$$

where in the first equality we have introduced the notation $b_{kl} = \ln^2(\mu^2/(-s_{kl})) = b_{lk}$ and $a_{ij} = \ln(\mu^2/(-s_{ij})) = a_{ji}$. In the second equality in Eq. (D5) we have identified the nonvanishing terms in the commutator, for which one and only one pair of generators is matched between the two entries of the commutator. Because the scalar products are symmetric, there are four ways in which this matching may occur, for fixed indices $i \neq j \neq k$. Finally, the third equality shows the result of performing the commutator explicitly for the generators on the j line. This form is reminiscent of the color structure of $\hat{\mathbf{H}}_{\mathrm{f}}^{(2)}$, Eq. (5.13), although the triple-logarithmic momentum factors are different, and depend on the renormalization scale μ.

To make contact between Eq. (D5) and the explicit expression (5.13) for $\hat{\mathbf{H}}_{\mathrm{f}}^{(2)}$, we convert the sum of unequal choices of i, j, and k into a sum over distinguishable triplets, denoted (i, j, k). For each such choice, there are six permutations of the indices i, j, and k in the final expression of Eq. (D5). These can be thought of as three cyclic permutations, which leave the structure constants the same, but change the momentum factors, and three more (exchanges of i and k for fixed j, plus cyclic permutations), which change the sign of the structure constants, and change the kinematic factors.

Following this path, we define

$$c_{[kj,ji]} \equiv b_{kj} a_{ji} - b_{ij} a_{jk} \tag{D6}$$

and rewrite $\mathcal{C}_{3,\mathrm{f}}$ as

$$\mathcal{C}_{3,\mathrm{f}} = \frac{1}{2}\sum_{(i,j,k)} i f_{a_1 a_2 a_3}\mathbf{T}_k^{a_1}\mathbf{T}_j^{a_3}\mathbf{T}_i^{a_2}\Big[c_{[kj,ji]} + c_{[ik,kj]} + c_{[ji,ik]}\Big]. \tag{D7}$$

A straightforward calculation shows that all of the μ dependence cancels in this expression. Relabeling the indices, and using the antisymmetry of the structure constants, we derive

$$\mathcal{C}_{3,\mathrm{f}} = -\frac{i}{2}\sum_{(i,j,k)} f_{a_1 a_2 a_3}\mathbf{T}_i^{a_1}\mathbf{T}_j^{a_2}\mathbf{T}_k^{a_3} \times \ln\!\left(\frac{-s_{ij}}{-s_{jk}}\right)\ln\!\left(\frac{-s_{jk}}{-s_{ki}}\right)\ln\!\left(\frac{-s_{ki}}{-s_{ij}}\right) = -\frac{1}{2}\hat{\mathbf{H}}_{\mathrm{f}}^{(2)}, \tag{D8}$$

which establishes the result of Eq. (5.18). We emphasize that, unlike our demonstration that $\mathcal{C}_{2,\mathrm{f}}$ vanishes, this result holds for an arbitrary $2 \to n$ process.

[1] A. Sen, Phys. Rev. D **28**, 860 (1983).
[2] J. Botts and G. Sterman, Nucl. Phys. **B325**, 62 (1989).
[3] N. Kidonakis, G. Oderda, and G. Sterman, Nucl. Phys. **B531**, 365 (1998).
[4] N. Kidonakis, G. Oderda, and G. Sterman, Nucl. Phys. **B525**, 299 (1998).
[5] N. Kidonakis and J. F. Owens, Phys. Rev. D **63**, 054019 (2001).
[6] A. Banfi, G. P. Salam, and G. Zanderighi, J. High Energy Phys. 08 (2004) 062.
[7] R. Bonciani, S. Catani, M. L. Mangano, and P. Nason, Phys. Lett. B **575**, 268 (2003).
[8] M. Dasgupta and G. P. Salam, Phys. Lett. B **512**, 323 (2001).
[9] G. Sterman and M. E. Tejeda-Yeomans, Phys. Lett. B **552**, 48 (2003).
[10] C. Anastasiou, E. W. N. Glover, C. Oleari, and M. E. Tejeda-Yeomans, Nucl. Phys. **B601**, 318 (2001); **B601**, 341 (2001); **B605**, 486 (2001); Z. Bern, A. De Freitas, and L. J. Dixon, J. High Energy Phys. 06 (2003) 028; E. W. N. Glover, J. High Energy Phys. 04 (2004) 021; A. De Freitas and Z. Bern, J. High Energy Phys. 09 (2004) 039.
[11] E. W. N. Glover, C. Oleari, and M. E. Tejeda-Yeomans, Nucl. Phys. **B605**, 467 (2001).
[12] Z. Bern, A. De Freitas, and L. J. Dixon, J. High Energy Phys. 03 (2002) 018.
[13] S. Catani and M. H. Seymour, Phys. Lett. B **378**, 287 (1996); Nucl. Phys. **B485**, 291 (1997); **B510**, 503(E) (1998).
[14] S. Catani, Phys. Lett. B **427**, 161 (1998).
[15] W. T. Giele and E. W. N. Glover, Phys. Rev. D **46**, 1980 (1992).
[16] Z. Kunszt, A. Signer, and Z. Trócsányi, Nucl. Phys. **B420**, 550 (1994).
[17] S. M. Aybat, L. J. Dixon, and G. Sterman, Phys. Rev. Lett. **97**, 072001 (2006).
[18] B. Jantzen, J. H. Kühn, A. A. Penin, and V. A. Smirnov, Nucl. Phys. **B731**, 188 (2005); **B752**, 327(E) (2006).
[19] L. W. Garland, T. Gehrmann, E. W. N. Glover, A. Koukoutsakis, and E. Remiddi, Nucl. Phys. **B627**, 107 (2002); **B642**, 227 (2002).
[20] Z. Bern, L. J. Dixon, and D. A. Kosower, J. High Energy Phys. 08 (2004) 012.
[21] R. Akhoury, Phys. Rev. D **19**, 1250 (1979).
[22] L. Magnea and G. Sterman, Phys. Rev. D **42**, 4222 (1990).
[23] L. Magnea, Nucl. Phys. B, Proc. Suppl. **96**, 84 (2001); Nucl. Phys. **B593**, 269 (2001).
[24] J. C. Collins, Adv. Ser. Dir. High Energy Phys. **5**, 573 (1989).
[25] R. J. Gonsalves, Phys. Rev. D **28**, 1542 (1983); G. Kramer and B. Lampe, Z. Phys. C **34**, 497 (1987); **42**, 504(E) (1989); T. Matsuura and W. L. van Neerven, Z. Phys. C **38**, 623 (1988); T. Matsuura, S. C. van der Marck, and W. L. van Neerven, Nucl. Phys. **B319**, 570 (1989).
[26] R. V. Harlander, Phys. Lett. B **492**, 74 (2000).
[27] S. Moch, J. A. M. Vermaseren, and A. Vogt, J. High Energy Phys. 08 (2005) 049; Phys. Lett. B **625**, 245 (2005).
[28] G. P. Korchemsky and A. V. Radyushkin, Nucl. Phys. **B283**, 342 (1987).
[29] I. A. Korchemskaya and G. P. Korchemsky, Nucl. Phys. **B437**, 127 (1995).
[30] J. Kodaira and L. Trentadue, Phys. Lett. **112B**, 66 (1982).
[31] A. Sen, Phys. Rev. D **27**, 2997 (1983).
[32] I. Balitsky, Phys. Rev. D **60**, 014020 (1999); T. Kucs, Phys. Rev. D **69**, 054016 (2004).
[33] N. Kidonakis, hep-ph/0208056.
[34] G. Sterman, in *Perturbative Quantum Chromodynamics*, edited by D. W. Duke and J. F. Owens (AIP, New York, 1981), p. 22; J. G. M. Gatheral, Phys. Lett. **133B**, 90 (1983); J. Frenkel and J. C. Taylor, Nucl. Phys. **B246**, 231 (1984); C. F. Berger, hep-ph/0305076.
[35] C. F. Berger, Phys. Rev. D **66**, 116002 (2002).
[36] S. Catani, B. R. Webber, and G. Marchesini, Nucl. Phys. **B349**, 635 (1991).
[37] L. J. Dixon, in *QCD & Beyond: Proceedings of TASI '95*, edited by D. E. Soper (World Scientific, Singapore, 1996).
[38] V. Ravindran, J. Smith, and W. L. van Neerven, Nucl. Phys. **B704**, 332 (2005).
[39] Yu. L. Dokshitzer and G. Marchesini, Phys. Lett. B **631**, 118 (2005); J. High Energy Phys. 01 (2006) 007; M. H. Seymour, J. High Energy Phys. 10 (2005) 029.
[40] A. Kyrieleis and M. H. Seymour, J. High Energy Phys. 01 (2006) 085.
[41] J. M. Cornwall and G. Tiktopoulos, Phys. Rev. D **15**, 2937 (1977); J. Frenkel and J. C. Taylor, Nucl. Phys. **B124**, 268 (1977).
[42] D. Binosi and L. Theussl, Comput. Phys. Commun. **161**, 76 (2004).
[43] J. A. M. Vermaseren, Comput. Phys. Commun. **83**, 45 (1994).